MODELING OF WIND AND RADAR FOR SIMULATION IN FOUR-DIMENSION NAVIGATION ENVIRONMENT

Gérard Malherbe

MIT

DEPARTMENT OF AERONAUTICS & ASTRONAUTICS

FLIGHT TRANSPORTATION LABORATORY
Cambridge, Mass. 02139

R76-8 September 1976

MODELING OF WIND AND RADAR FOR SIMULATION IN FOUR-DIMENSION NAVIGATION ENVIRONMENT

by

Gérard Malherbe

Flight Transportation Laboratory
Massachusetts Institute of Technology
Department of Aeronautics and Astronautics
Cambridge, Massachusetts 02139

FTL Report R76-8
September, 1976

ACKNOWLEDGEMENT

I would like to express my gratitude to the people who made this study possible:

to Professor Robert W. Simpson, my advisor, for his counsel and encouragement;

to Mark Connelly, Research Engineer, for his invaluable comments on air traffic control;

to the Flight Transportation Laboratory for making this work materially possible;

to the faculty and staff of M.I.T. and particularly to the librarians, whose support has been essential to the success of this study.

ABSTRACT

Disturbances affecting time control precision in four-dimension navigation are modeled. Several models of wind and turbulence from the ground to ten thousand feet are developed. A distinction is made between wind mean and turbulence and between the different layers of the troposphere. These models can be used for most cases of flight simulations. A selection of simple wind and radar models is made. Real-time computer programs using a mathematical model of a Boeing 707-320B are developed.

TABLE OF CONTENTS

Table of Contents

LIST OF SYMBOLS

C_p	Specific heat at constant pressure
f	Coriolis parameter, $f = 2\omega_E \sin\psi$
g	Acceleration due to gravity
k	Von Karman constant, $k = 0.35$
K_u, K_θ	Turbulence coefficients
L, L'	Monin Obukhov scaling length and modified scaling length
L_T, L_H, L_V	Integral scales for turbulence and, horizontal and vertical components, respectively
p, p_r, p'	Pressure, reference pressure, deviations from reference pressure, respectively
q	Vertical turbulent heat flux
r	Radius of isobars
R	Gas constant
R_f	Flux Richardson's number
R_i	Gradient Richardson's number
R_{ij}	Correlation function
s	Nondimensional wind shear $\left(s = \frac{kz}{u_{*_0}} \frac{\delta \bar{u}}{\delta z}\right)$
S	Spectral density
t	Time
T, T_r, T', T_0	Temperature, reference temperature, deviations from reference temperature, and standard temperature, respectively

T_*	Monin Obukhov temperature scale
u, v, w	Velocity components along x, y, z respectively
u_r, v_r, w_r	Components of reference velocity along x, y, z, respectively
u_T, v_T, w_T	Turbulence velocity components along x, y, z, respectively
u', v', w'	Components of deviation from reference velocity along x, y, z, respectively
u_*, u_{*_0}	Friction velocity and friction velocity at the surface, respectively
V_a	Aircraft airspeed
V_g	Geostrophic wind speed
x, y, z	Position components
x_m, y_m, z_m	Measured aircraft position components
x_R, y_R, z_R	Radar position components
z_{BL}, z_{SL}	Altitudes of the boundary layer and surface layer, respectively
z_{ref}	Reference altitude: measure of mean wind $\bar{u}$ ref
z_0	Roughness length
α, α_0	Angle wind/geostrophic wind and surface wind/geostrophic wind, respectively
α_{SL}	Shift angle at the top of the boundary layer
β	Buoyancy ($\beta = g/T_0$)
β_1	Constant of Deacon profile
Δ_n	Load factor variation
Δ_t	Sampling period

δ_{ij}	Kronecker function
$\bar{\xi}_{\theta}$	Displacement vector
θ_a, ρ_a, θ_m, ρ_m	Polar coordinates of the aircraft: absolute (a), measured (m)
θ_p	Potential temperature
ρ, ρ_r, ρ', ρ_0	Density, reference density, variation from reference density and standard density, respectively
σ_H, σ_v	Standard deviation of horizontal and vertical turbulence, respectively
σ_u, σ_v, σ_w	Standard deviation of u_T, v_T, w_T, respectively
τ, τ_x, τ_y, τ_z	Turbulence shear stress: module and components along x, y, z, respectively
ϕ	Latitude
Φ_{ij}	Power spectrum
Φ_{NN}, Φ_{pp}	Transversal and longitudinal power spectra, respectively
Φ	Bank angle
Ψ, Ψ_w	Aircraft and wind headings, respectively
Ω, Ω_1, Ω_2, Ω_3	Spacial frequency: magnitude and components
ω	Temporal frequency
ω_E	Earth rotation

CHAPTER I

INTRODUCTION

1.1 Four-Dimension Navigation Environment

All over the world, big airports are facing the problem of increasing demand. New concepts in Air Traffic Control must be introduced to solve this problem. Not only is the demand dramatically increasing, but higher levels of safety and reductions of costs are needed.

A growth of the size of Air Traffic Control services cannot be considered as a satisfactory solution; the situation is now such that the marginal benefit of size increase of these services is almost negligible. Therefore new methods of time and space management must be found. Furthermore, the problem of energy management must not be forgotten.

Many airports are now saturated several hours a day. The consequences of this situation on safety and costs are not acceptable. The origin of the problem is dual: airspace and runways. In order to maximize runway efficiency a new approach of air traffic control in the terminal area is needed.

Present Air Traffic Control procedures use primarily heading and speed commands to the aircraft called radar vectoring. In this system aircraft arrive randomly at the boundary of the terminal area. It is possible to derandomize this flow if aircraft are controlled earlier, and are requested to report at certain points at given times. This

new concept of waypoints associated with a time characterizes Strategic Navigation, also called Four-Dimension Navigation.

In fact Strategic Navigation can be applied only in the terminal area, at an effective cost. There is really a trade-off between accuracy and efficiency.

This terminal area concept allows a good management of energy, space and runways. The principle of the method is to assign a route-time profile to every aircraft. This can be done by transmitting the desired route-time profile from the ground to the aircraft. In this case, an airborne system using precision four-dimensional navigation and guidance equipment is entirely repsonsible for carrying out the commands. Another method, favored by the Federal Aviation Administration (FAA), consists of giving commands (heading, speed, etc.) from the ground.

All combinations of these two methods are also possible, but in all cases, Four-Dimension Navigation can be split into two parts:

- determine a route-time profile
- carry out this route-time profile.

Therefore, two controllers must be designed:

- a scheduler which assigns waypoints and times to the aircraft
- a 4-Dimension Strategic Navigation Controller which gives commands to the aircraft in order to carry out the schedule.

The scheduler and the navigation controller use aircraft models to generate their commands. These models should be as simple as possible because they are used in real time computations. However, a question

arises: is it necessary to build a complex model of disturbances and, especially, wind? Many methods of wind estimation are now available from simple regression to applications of realization theory to the "wind process" (see for instance the very interesting study of Menga and Sundararajan, 1976).

In order to test these algorithms a sophisticated simulation is necessary. It is first necessary to design a very accurate aircraft model. This accuracy is required to test efficiently the controllers which use simpler models of the aircraft. Furthermore, a model for disturbances must also be provided for the simulation to test the scheduler and navigation controller.

The purpose of this study is to model the disturbances affecting strategic navigation. After a short review of the aircraft model in 1.2 and of these disturbances in 1.3, the models will be described in detail in Chapters II, III, and IV.

1.2 The Aircraft Simulation

The simulation facilities consist of a fixed-base cockpit simulation roughly similar to a Boeing 707 cockpit (see Figures 1.1 and 1.2). The cockpit is interfaced with an Adage AGT-30 digital computer which drives the flight instruments using CRT's. A block diagram of the simulation facilities is shown in Figure 1.3.

The modeled aircraft is a Boeing 707-320B. This plane was selected because many data on this plane were available and also because it was widely used.

The model is a nonlinear model developed at M.I.T. by Corley (1974)

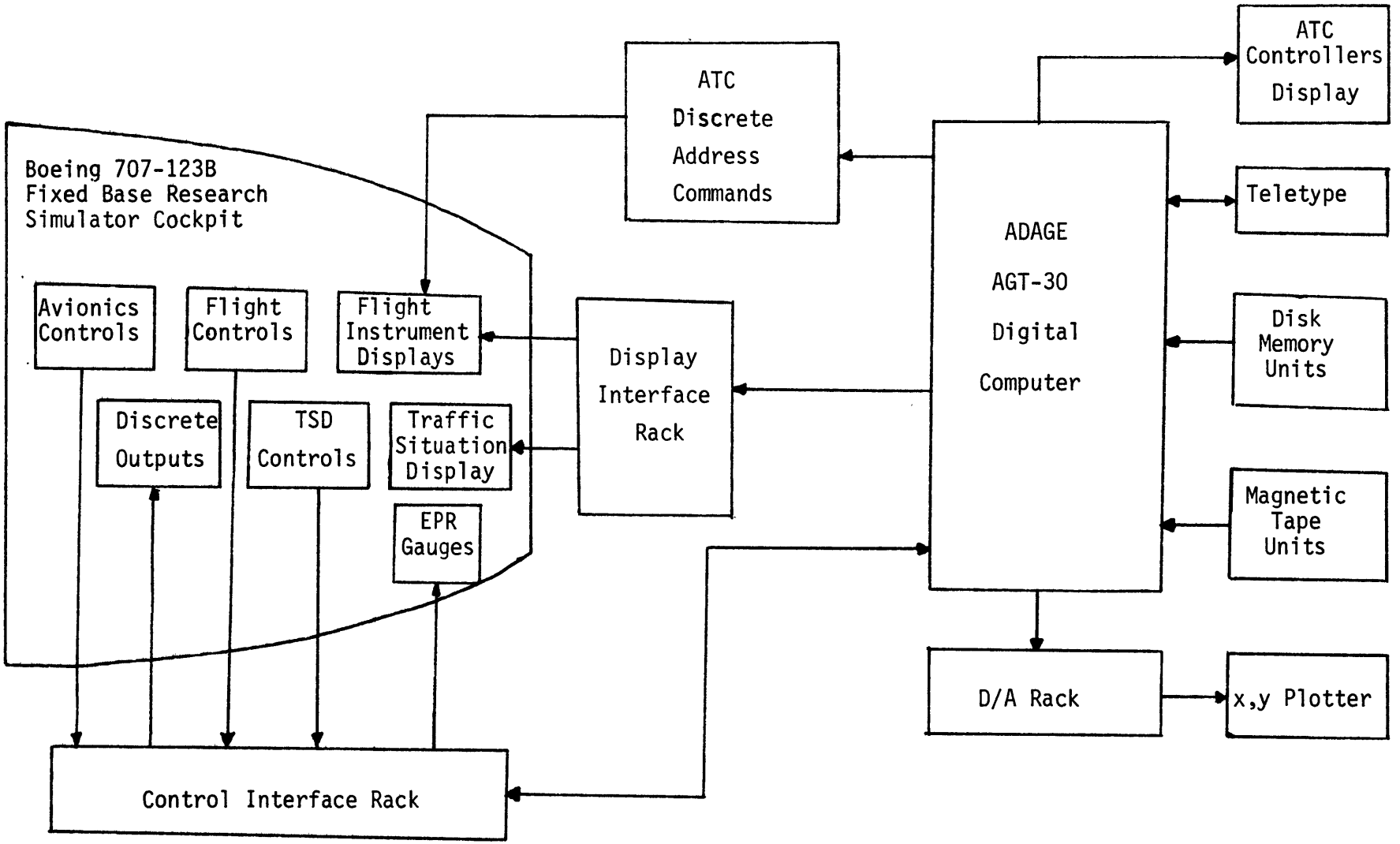

Figure 1.3: Simulation Facilities

and then by Lax (1975). The derivation of the model is classical and will not be examined in detail in this study. In Chapter IV we will deal more particularly with the connections of this model with the other models used.

1.3 Disturbances Affecting Time Control Precision

The purpose of this study is to simulate the flight of an aircraft in a Four-Dimension Navigation Environment. More precisely, we will simulate a system in which position is estimated from noisy ground radar observations. The speed is also estimated from these observations. Therefore, the radar errors are one of the sources of disturbance, or noise for time control precision.

The navigation controller computes the required speed for every aircraft knowing positions and scheduled times at waypoints. It is then clear that low frequency variations of wind will induce errors in time estimates. Thus, a model of the wind will be studied to estimate the influence of these disturbances. The emphasis will be put on slowly varying winds which are much more important than high frequency turbulence for time control accuracy.

A study of the disturbances affecting time control accuracy was also made by the Collins Radio Company (Hemesath et al., 1974). This study covers the descent through a known wind, time dispersion due to correlated wind errors and prediction of timing dispersion at touchdown for open loop control from the outer marker to the ground (approximately five miles). The selected models are very simple. Wind variations with time and horizontal displacement were neglected for the study of

descent through known winds. The models are just records of observed data. For a descent from 20,000 feet to the ground with a 2000 ft/min descent rate, they get a standard deviation of six nautical miles. It goes down to 2 nautical miles if a linear profile of wind velocity (interpolation or constant velocity) is used for compensation. At 120 knots, this error is 60 seconds expressed as a time error. The effect of wind errors is also estimated. Wind is modeled as a random process with horizontal and vertical correlation distances of 50 to 100 and 3 nautical miles, respectively. The dispersion is estimated at 1 to 3 seconds per knot of wind in the final area. The effect of wind shear is estimated at 8 seconds (standard deviation) from the outer marker to the threshold.

This study provides a good idea of the magnitude of the errors. However, the models used are too simple to examine different meteorological situations and not useful to test pilots, for instance.

The study developed here is specially adapted for implementation in a flight simulation. The models are designed to be "flown" in real time by pilots. Wind models are first examined in detail in Chapters II and III. In chapter IV the implementation of all the models in the simulation is discussed.

CHAPTER II

MEAN WIND MODEL

2.1 Introduction

The distinction is generally made between mean wind and turbulence. Some people consider another category: gusts. In this study gusts are considered as a component of turbulence, the other being lulls. "Discrete" gusts, that is to say sudden and individual gusts, due to local phenomenon, will not be taken into account.

To define a mean wind is rather difficult. This mean must be the average over a certain amount of time, and this average should be independent of the interval chosen.

We will choose a statistical point of view to make the distinction between mean wind variations and turbulence. Many observations (Van der Hoven 1957, Vinnichenko 1970, Fiedler and Panofsky 1970) show that there is a gap in the power spectrum of the wind speed. The very well known Van der Hoven spectrum of horizontal wind speed is shown in Figure 2.1.

This gap is not an original case, it seems that there is always a gap from 15 minutes to 2 or 3 hours. This gap has two advantages: distinction between turbulence and mean speed and possibility of averaging.

All the variations corresponding to frequencies higher than the gap will be called turbulence. They correspond to the micrometeorological scale. All the variations corresponding to frequencies lower than the gap will be called mean wind variations. They correspond to the mesometeorological scale.

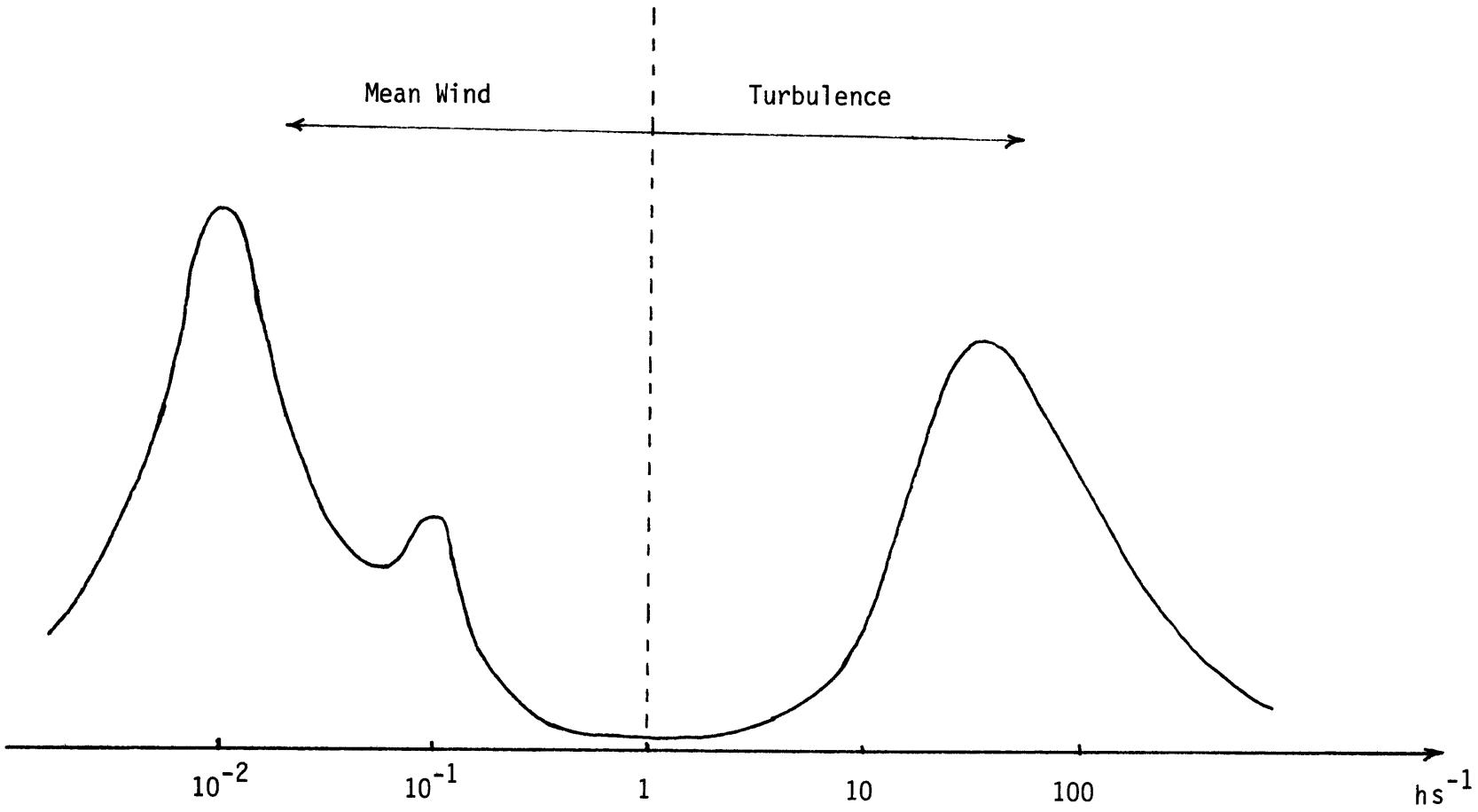

Figure 2.1: Power Spectrum of Wind Van der Hoven 1957

If we choose the averaging period in this gap, the filtered energy is approximately independent of this gap. Furthermore, in these conditions, an averaged quantity, which is a function of time, is invariant by averaging (Tverskoi, 1965) which is absolutely necessary in order to have a stable system of equations.

Let us denote u the instantaneous value of the wind velocity, then if u' is defined by

$$u'(x,y,z,t) = u(x,y,z,t) - \bar{u}(x,y,z,t)$$

this property of idempotence of the average is simply

$$\overline{u'(x,y,z,t)} = 0$$

In the last equation, the average is a time average and therefore it is a function of the location. However, in our study we need a wind independent of the location and therefore we also have to take the average on the spatial coordinates. In order to solve this problem we will make another hypothesis, the ergodic hypothesis. It means that the average with respect to time is the same as the average with respect to space.

It is very difficult to test this hypothesis which is generally accepted. The equivalence of probability means, time means and space means (ergodicity) can be "proven" with the aid of random processes theory (see for instance, Monin and Yaglom, 1971).

In this chapter we will build a model for the wind mean. Since we are only interested in the micrometeorological scale, this mean will be independent of time. This model will describe the variation of the wind with altitude from the ground to ten thousand feet.

This wind profile giving the strength and the direction of wind for every altitude, will also give the wind shear. That is to say, the gradient of wind speed with respect to altitude. This wind shear is the more important effect of wind variations on time control in a 4-Dimension Navigation situation.

2.2 A Theoretical Approach to Wind Modeling

2.2.1 Introduction

The physical properties of atmosphere are nonuniform. By the criteria of interaction with the earth's surface, the atmosphere is divided into the boundary layer (or the friction layer or the Ekman layer) and the free atmosphere. In fact, the boundary layer itself is divided into the surface layer and the rest which is merely called the boundary layer. The surface layer is a constant flux layer close to the ground in which the vertical fluxes of heat, momentum and moisture are invariant with height, and the Coriolis forces are unimportant. The height of the surface layer is typically 300 feet and will be discussed in more detail in 2.3.

The boundary layer is the layer above the surface layer in which the motion is influenced by the underlying surface and turbulent friction. Its height is considerably variable; it can go up to more than 4000 feet and will be discussed in 2.4.3.

2.2.2 The Basic Equations

The equations governing fluid flows are the non-linear Navier-

Stokes equations (Landau and Lifchitz 1971). However, these equations are too difficult to be solved and are generally replaced by the so-called Boussinesq equations (Oberbeck 1879, Boussinesq 1903).

The original set of equations consists of three equations for conservation of momentum (Navier-Stokes), an equation for conservation of mass (continuity equation), a thermodynamic energy equation (entropy equation), and an equation of state.

The Boussinesq equations are:

$$\frac{du_i}{dt} = -\frac{1}{\rho_0}\frac{\partial p'}{\partial x_i} + \nu\nabla^2 u_i + \beta T'\delta_{3i} + fu_2\delta_{i1} - fu_1\delta_{2i} \qquad (2.1)$$

for $i = 1,2,3$ (conservation of momentum)

$$\frac{\partial u_1}{\partial x_1} + \frac{\partial u_2}{\partial x_2} + \frac{\partial u_3}{\partial x_3} = 0 \qquad \text{(continuity equation)} \qquad (2.2)$$

$$\frac{dT'}{dt} = \gamma_\theta \nabla^2 T' \qquad \text{(entropy conservation)} \qquad (2.3)$$

$$\frac{\rho'}{\rho_0} = -\frac{T'}{T_0} \qquad \text{(state equation)} \qquad (2.4)$$

In these equations x_1, x_2, x_3 represent x, y, z respectively (z positive upwards), the position, and u_1, u_2, u_3 represent u, v, w respectively (components of wind speed). The variables ρ', p', T' represent the deviations from the reference state ρ_r, p_r, T_r :

$$\rho = \rho_r + \rho' \; ; \qquad p = p_r + p' \; ; \qquad T = T_r + T'$$

The reference is defined by:

$$p_r = \rho_r R T_r \; ; \qquad \frac{\partial p_r}{\partial z} = - \rho_r g \; ; \qquad \frac{\partial T_r}{\partial z} = - \frac{g}{C_p}$$

(ideal gas) (hydrostaticity) (adiabaticity)

and is only a function of z.

All the other symbols have their usual meanings and are defined in the "List of Symbols".

To get these equations it is assumed that

- the dynamic viscosity $\mu = \rho\nu$ is constant
- the molecular conductivity is constant
- $|\rho'/\rho_r| \ll 1$
- $|T'/T_r| \ll 1$
- $|p'/p_r| \ll 1$
- the heat generated by viscous stresses is neglected
- the vertical scales of motion are small compared to $|\frac{1}{\rho_r} \frac{\partial \rho_r}{\partial z}|^{-1}$ (scale height) : shallow convection.

The derivation of these Boussinesq equations is very difficult (Calder 1968, Dutton and Fichtl 1969) and is only a first step to build the model. These equations (2.1 to 2.4) represent the smallest scale at which the air can be considered as continuous. This means that the variables are indeed averages on a domain very large compared to

molecular dimensions, but very small compared to the scale of the smallest eddies. This domain defines a scale known as the laboratory scale.

In order to get a model for the micrometeorological scale, we need to average these equations. This is possible because of the existence of a gap in the spectrum of wind velocity (see 2.1).

We will also make the hypothesis of horizontal homogeneity ($\frac{\partial}{\partial x} \equiv \frac{\partial}{\partial y} \equiv 0$ for all average variables except pressure) and stationarity ($\frac{\partial}{\partial t} \equiv 0$). In fact it is only quasi-homogeneity and quasi-stationarity since we only exclude an explicit dependence on x, y, and t.

In the case of average horizontal pressure, gradient independent of altitude, the Boussinesq equations become:

$$\bar{w} = 0 \qquad \text{(continuity)}$$

$$T' = \theta_p - T_0 \qquad \begin{cases} \theta_p \text{ - potential temperature} \\ T_0 \text{ - standard temperature} \end{cases} \qquad (2.5)$$

$$\frac{\partial}{\partial z} (\overline{w'u'} - \gamma \frac{\partial \bar{u}}{\partial z}) - f (\bar{v} - v_g) = 0 \qquad (2.6)$$

$$\frac{\partial}{\partial z} (\overline{w'v'} - \gamma \frac{\partial \bar{v}}{\partial z}) + f (\bar{u} + u_g) = 0 \qquad (2.7)$$

$$\frac{\partial}{\partial z} (\overline{w'\theta_p'} - \gamma_\theta \frac{\partial \bar{\theta}_\rho}{\partial z}) = 0 \qquad (2.8)$$

u', v', w' are the deviations from the means $\bar{u}$, $\bar{v}$, $\bar{w}$ and u_g, v_g are the components of the geostrophic wind ($u_g = - \frac{1}{\rho_0} \frac{\partial \bar{p}}{\partial y}$, $v_g = - \frac{1}{\rho_0} \frac{\partial \bar{p}}{\partial x}$,

ρ_0 : standard density).

The problem is that we do not have enough equations: we need to know the moments $\overline{w'u'}$, $\overline{w'v'}$, $\overline{w'\theta'}$. The easiest way to solve that problem is to introduce some coefficients known as turbulence coefficients:

$$\overline{w'u'} = -K_u \frac{\partial \bar{u}}{\partial z} \tag{2.9}$$

$$\overline{w'v'} = -K_u \frac{\partial \bar{v}}{\partial z} \tag{2.10}$$

$$\overline{w'\theta'_p} = -K_\theta \frac{\partial \bar{\theta}_\rho}{\partial z} \tag{2.11}$$

This approach is very empirical but has the great advantage of yielding simple results which are in accordance with experimental data. These equations either in their original form (de Moor 1976) or with the turbulence coefficients approach are used for wind simulation. They allow us to compute the state of the atmosphere from point to point (grid simulations) or to develop some semi-empirical models (see next section).

2.2.3 The Similarity Theory

Atmospheric physics and turbulent flows physics make a large use of dimensional analysis. These methods are used when the differential equations describing a phenomenon cannot be solved.

The basic theorem of this theory is the so-called "Π-theorem". According to this theorem, a relation between n + 1 dimensional quantities

$b_1, b_2, \ldots, b_n$, which is independent of the choice of the system of units, can be represented as a relation between n + 1 - k quantities $\Pi, \Pi_1, \Pi_2, \ldots, \Pi_{n-k}$ which are dimensionless combinations of the n + 1 dimensionless quantities, of which k is dimensionally independent (see Matveev 1967, for instance).

The similitude theory (or similarity theory) allows us to know the variables on which a given quantity depends. Two processes are called similar if any quantity describing a process is proportional to a "similar" quantity of the other process. The proportionality factor (similarity constant) must be independent of position and time.

The "direct theorem of the theory of similitude" states that if processes are similar to one another, their similarity criteria (the dimensionless combinations Π_i) have the same values and the processes themselves are described by the same similarity equation.

The most important application of this theory to atmospheric physics is the Monin-Obukhov similarity theory (Monin-Yaglom 1971). This theory covers both the case of neutral stratification and the more realistic case of thermal stratification, that is, when temperature varies with height. The flow in a thermally stratified medium is described by equations (2.1)(in which the Coriolis forces are neglected), (2.2), (2.3), (2.4), and the conditions:

$$-\rho_0 \overline{u'w'} + \rho_0 \nu \frac{\partial \bar{u}}{\partial z} = \tau = \text{constant} \qquad (2.12)$$

(approximation of (2.1) averaged)

$$C_p \rho_0 \overline{w'T'} - C_p \rho_0 \gamma_\theta \frac{\partial \bar{T}}{\partial z} = q = \text{constant} \qquad (2.13)$$

(equation (2.3) averaged in steady conditions).

Therefore, the flow depends on the parameters β, ρ_0, ν, γ_θ, τ, q and on the roughness parameter z_0, which describes the ground surface (boundary conditions). ν and γ_θ are molecular coefficients and can be ignored (fully rough flow). Equations (2.12) and (2.13) become;

$$-\rho_0 \overline{u'w'} = \tau = \text{constant} \tag{2.14}$$

$$C_p\rho_0 \overline{T'w'} = q = \text{constant} \tag{2.15}$$

The state of the atmosphere at a given height depends upon the boundary conditions characterized by the coefficient z_0. However, the vertical variation of the mean parameters should not depend on z_0; the effect of z_0 is only a shift of the curves $\bar{u}(z)$ and $\bar{T}(z)$ if $z \gg z_0$.

Therefore, we have only four parameters:

- density
- turbulent shear stress τ (or $u_* = \sqrt{\frac{\tau}{\rho_0}}$: friction velocity)
- vertical turbulent heat flux q (or $q/C_p\rho_0$)
- buoyancy $\beta = \frac{g}{T_0}$

In the case of neutral stratification, $q = 0$ and therefore, there is no buoyancy; the buoyancy parameter $\frac{g}{T_0}$ disappears.

The turbulence characteristics depend upon five quantities, z, ρ_0, $\frac{g}{T_0}$, u_*, and $\frac{q}{C_p\rho_0}$. Applying the "direct theorem of the theory of similitude", we can form only one independent combination with these five parameters (there are, of course, four independent dimensions: length, time, mass and temperature).

Monin and Obukhov chose the following combination:

$$\zeta = \frac{z}{L} \tag{2.16}$$

where

$$L = - \frac{u_*^3}{k \frac{g}{T_0} \frac{q}{C_p \rho_0}} \tag{2.17}$$

k is the dimensionless von Karman constant. Its value is approximately 0.4 or 0.35 (Businger et al. 1971). The sign of L is chosen so that $L > 0$ for stable thermal stratification ($q > 0$).

So, any characteristic of the atmosphere ψ is described by an equation of the form:

$$\bar{\psi}(z) = \psi_0 F(\zeta)$$

where F is a universal function.

Then if for the temperature scale we take

$$T_* = - \frac{1}{k u_*} \frac{q}{C_p \rho_0} \tag{2.18}$$

we get the following equations:

$$\frac{\partial \bar{u}}{\partial z} = \frac{u_*}{kL} g(\zeta) \tag{2.19}$$

$$\frac{\partial \bar{T}}{\partial z} = \frac{T_*}{L} g_1(\zeta) \tag{2.20}$$

where g and g_1 are two universal functions.

$g(\zeta)^{-1}$ is known as the flux Richardson number R_f:

$$R_f = - \frac{g}{C_p T_0} \frac{q}{\tau \frac{\partial \bar{u}}{\partial z}} \tag{2.21}$$

The more classical Richardson number R_i can also be expressed with the aid of g and g_1:

$$R_i = \frac{g}{T_0} \frac{\partial T/\partial z}{(\partial \bar{u}/\partial z)^2} = \frac{g_1(\zeta)}{g(\zeta)} \qquad (2.22)$$

More practically R_i is an index of the degree of development of turbulence. Experimental investigations yield:

* $R_i > 5 - 10$: calm
* $0.5 < R < 5$: slight bumpiness ($|\Delta n| \leq 0.2$ g)
* $R < 0.5$: moderate to strong bumpiness ($|\Delta n| \geq 0.2$ g)

Many experimental and theoretical investigations were made to determine approximations of the universal functions g and g_1 (Monin and Yaglom 1971, Zilitinkevitch 1973, Wyngaard 1973, Businger 1973, Lewellen and Teske 1973). These investigations have given birth to many wind models. However, it seems that at least for the "asymptotic" models (one parameter disappears), results are not very good for the correlations with u'. On the contrary, excellent models were obtained for the variation of $\overline{T'w'}$ (Wyngaard 1973).

2.3 Survey of Wind Profile Models in the Boundary Layer

We will derive some models for the mean wind profile; some valid only in the surface layer, some in the boundary layer in its strict sense (above the surface layer). For each model an idea of how this model is derived will be given. The accent will be put on the validity

domains and on the advantages and disadvantages of each one.

In this survey, we will deal only with the models which can be used for a real time simulation. That means that the grid models of the atmosphere will not be treated (models in which the computation is made point by point on a grid).

2.3.1 Logarithmic Profile (Prandtl)

The logarithmic wind profile is only valid in the surface layer; it is indeed the most widely used profile for this layer. In the surface layer, it has been observed that the mean wind has a direction approximately constant. This direction will be chosen for the x axis. In the case of neutral stability the Monin-Obukhov similitude theory (2.2.3) simply yields:

$$\frac{\partial \bar{u}}{\partial z} = \frac{u_*}{k(z + z_0)} \tag{2.23}$$

and by integration:

$$\bar{u} = \frac{u_*}{k} \ln\left(\frac{z + z_0}{z_0}\right) \tag{2.24}$$

$u_* = \sqrt{\frac{\tau}{\rho_0}}$ is difficult to estimate.

Since at airports the wind speed u is generally known at a reference altitude z_{ref} (usually 20 feet), the equation (2.24) can be written:

$$\bar{u} = \bar{u}_{ref} \frac{\ln\left(\frac{z + z_0}{z_0}\right)}{\ln\left(\frac{z_{ref} + z_0}{z_0}\right)} \tag{2.25}$$

(The approximation has been made that $u_* \approx u_{*_0}$.)

The only unknown parameter is z_0, the roughness length. This length characterizes the roughness of the ground. (For data on roughness length for different surfaces, see Huschke 1959, Nikuradse 1933). We will choose $z_0 = 0.15$ foot, value recommended by the British Air Registration Board for airports. The domain of validity for altitude is also very controversial. It seems that this model is a good approximation (around 10%) for altitudes as high as 300 feet. The approximations are better with u_{*_0} (Eq. 2.25) than with u_* (Eq. 2.24).

The characteristics of the logarithmic profile are:

- wind direction independent of altitude
- wind speed profile given by $\bar{u} = \bar{u}_{ref} \dfrac{\ell n\left(\dfrac{z + z_0}{z_0}\right)}{\ell n\left(\dfrac{z_{ref} + z_0}{z_0}\right)}$

  we take $z_0 = 0.15$ foot
- validity from 2 feet to 300 feet
- valid only in neutral thermal stratification
- fast and easy computation on a real time computer
- very simple use: only one parameter, the mean wind speed at a reference altitude

The wind profile and the mean wind shear profile for the model are plotted in Figures 2.2 and 2.3.

2.3.2 Extensions from the Logarithmic Profile

The principal shortcoming of the logarithmic profile is that it is only valid for stable conditions. Therefore, many other models were

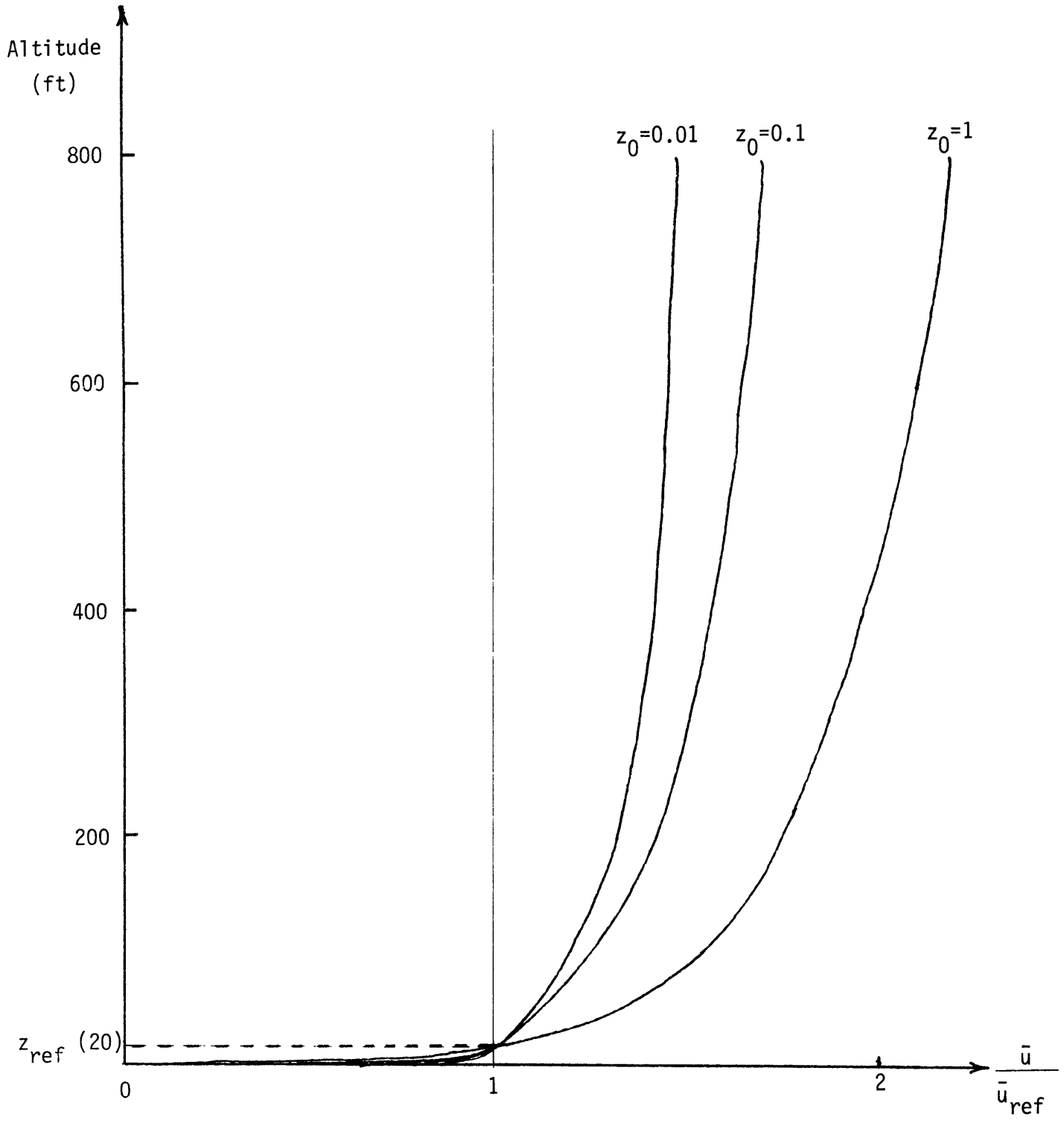

Figure 2.2: Logarithmic Mean Wind Profile

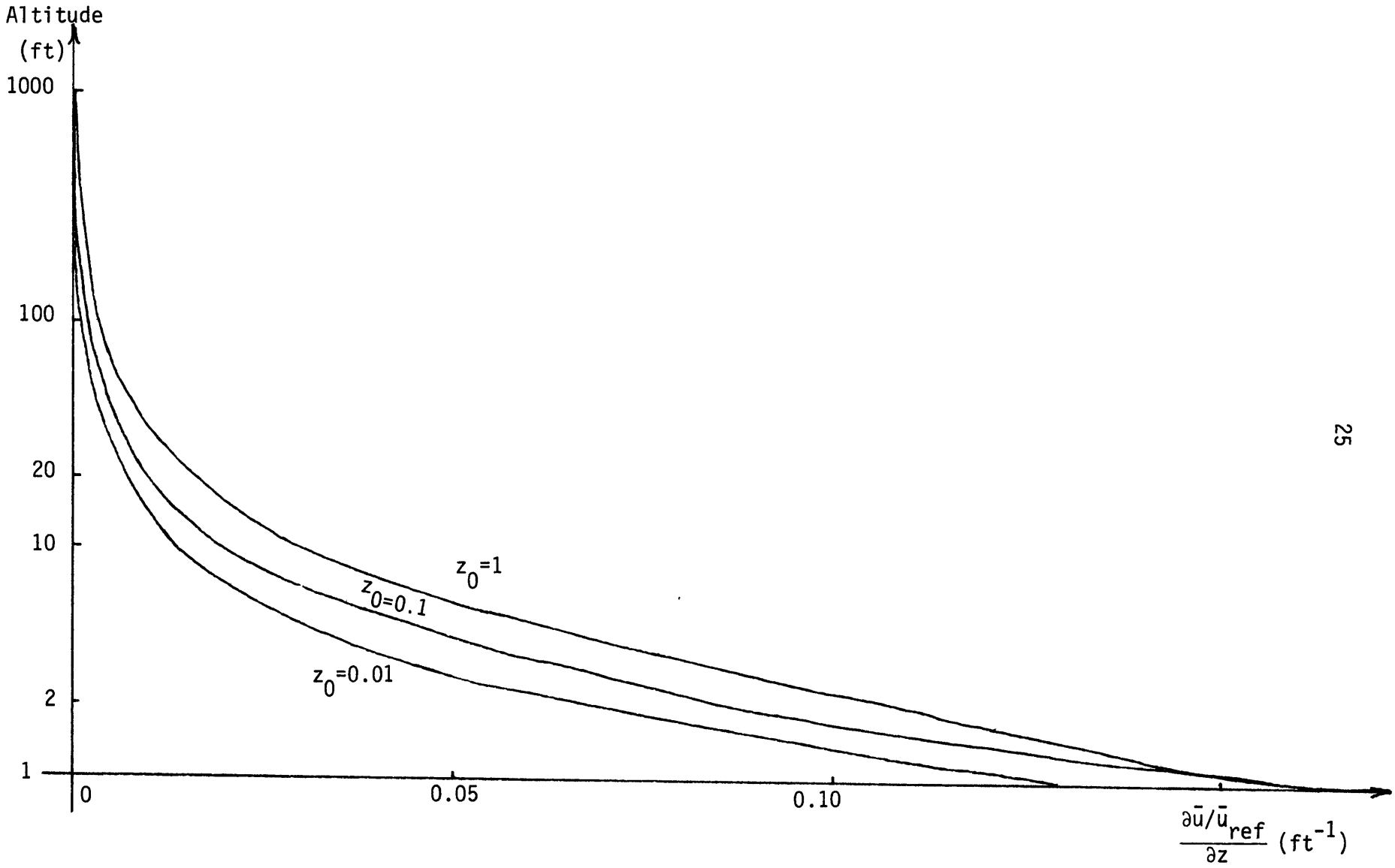

Figure 2.3: Mean Wind Shear (Log Model)

developed to deal with non-adiabatic conditions. Most of them are applications of Monin-Obukhov similarity theory with different universal functions.

The simpler and more well known is the log-linear profile which states that:

$$\begin{cases} \dfrac{\partial \bar{u}}{\partial z} = \dfrac{u_{*_0}}{k(z + z_0)} \left[1 + \alpha \left(\dfrac{z + z_0}{L} \right) \right] & (2.26) \\ \bar{u} = \dfrac{u_{*_0}}{k} \left[\ell n \left(\dfrac{z + z_0}{z_0} \right) + \alpha \dfrac{z}{L} \right] & (2.27) \end{cases}$$

The wind and wind shear profiles for this model are plotted on Figures 2.4 and 2.5. In fact L is generally replaced by another scaling length L' given by:

$$L' = \frac{u_{*_0} \, \theta (\partial \bar{u}/\partial z)}{kg \, (\partial \theta_p / \partial z)} \qquad (2.28)$$

z/L' and the Richardson's number (Eq. 2.22) are related by

$$R_i = \frac{z/L'}{1 + \alpha' \, z/L'}$$

$$z/L' = \frac{R_i}{1 - \alpha' \, R_i}$$

α' is a new coefficient such that $\frac{\alpha}{L} = \frac{\alpha'}{L'}$.

For small Richardson's numbers the equation of the profile becomes:

$$\bar{u} = \frac{u_{*_0}}{k} \left[\ell n \left(\frac{z + z_0}{z_0} \right) + R_i \right] \qquad (2.29)$$

The constant α' is generally taken equal to 4.5 although it depends

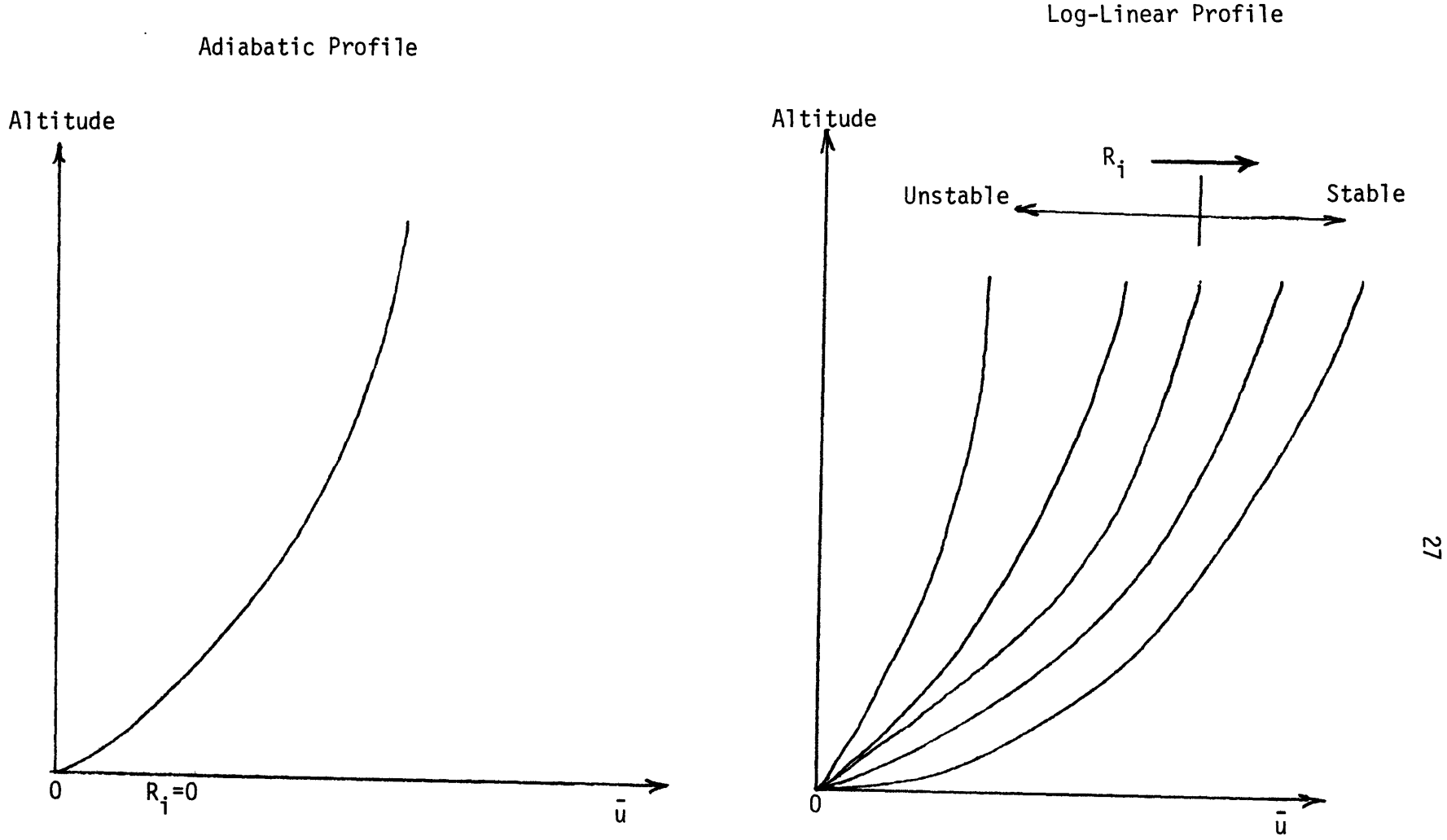

Figure 2.4: Wind Profile (Log-Linear Model)

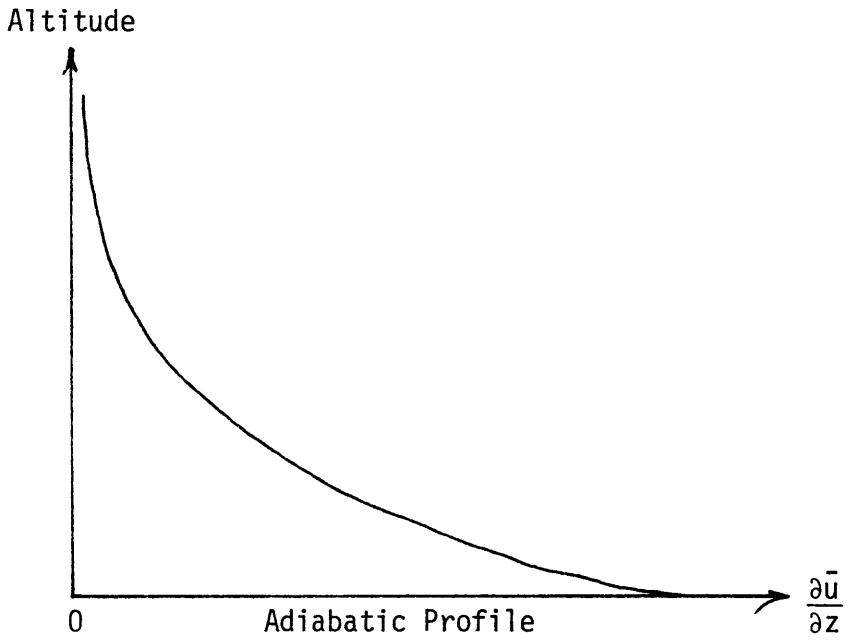

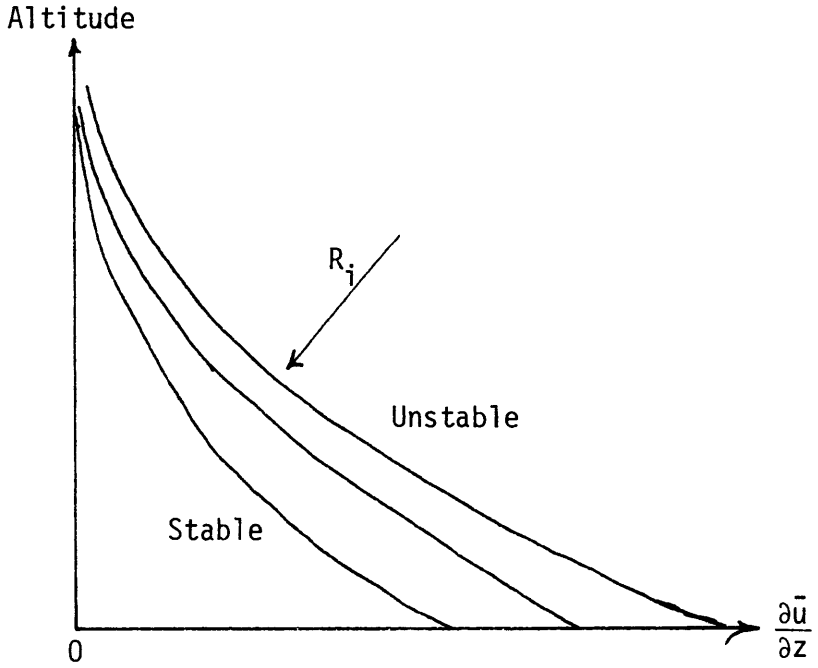

Figure 2.5: Mean Wind Shear (Log-Linear Model)

slightly on the atmospheric conditions.

This model is only valid for Richardson's numbers less than 0.16 (Webb, 1970): it is not valid for strong stability. In fact, it is also a poor approximation for moderate instability.

To solve the problem of limited range of stability, the so-called Keyps equation is used:

$$s^4 - \frac{\gamma' z}{L'} s^3 = 1 \tag{2.30}$$

where s is the nondimensional wind shear:

$$s = \frac{kz}{u_{*_0}} \frac{\partial \bar{u}}{\partial z} \tag{2.31}$$

This yields a wind profile given by:

$$\bar{u} = \frac{u_{*_0}}{k} \ln \frac{z + z_0}{z_0} + f(\frac{z}{L'}) \tag{2.32}$$

where f is a universal function given by an integral. This model gives a very good approximation of the wind profile. However, it is not valid for strong stability and supposes a constant wind direction in the surface layer (which sometimes turns up to 45° in the first 300 feet in very stable conditions). Furthermore, this model requires the computation of the universal function by integration, but since this can be done off-line, it is not very important.

An attempt to find a wind shear profile for all stability conditions has been made by Deacon. This profile is described by a unique equation:

$$\frac{\partial \bar{u}}{\partial z} = cz^{-\beta_1}$$

where c and β_1 depend only on stability. Unfortunately β has been found to vary with height.

Many other models just integrate the equation of wind shear (Eq. 2.23) assuming that it is not constant but varies with altitude according to a law dependent on stability. This is, for example, the case of the exponential-logarithmic profile of Izevkov (Matveev, 1965). These models are more and more complicated because they try to use algebraic relationships instead of more experimental universal functions.

2.3.3 The Power Law

Among all the empirical models available, one of the most simple and widely used is the power law. It is only a simple extrapolation of the wind speed:

$$\bar{u} = \bar{u}_{ref} \left(\frac{z}{z_{ref}} \right)^p \qquad (2.33)$$

The power law can be considered as an empirical relationship and also as an asymptotic approximation of the logarithmic profile. This law can be derived from the logarithmic case if the roughness length z_0 is much smaller than the reference altitude z_{ref} and if the wind speed is not too different from the wind speed at the reference level. Therefore it seems that all the restrictions applied to the logarithmic profile apply to the power law. Many investigations of the value of the exponent p have been made. It has been found that the best value is dependent on the roughness of the ground and varies from 1/2 to 1/10, 1/7 being the more used.

At altitudes higher than, say 200 feet, the power law begins to deviate significantly from the logarithmic profile. But neither one nor the other is significantly better, even in adiabatic conditions.

2.3.4 Wind Direction Shifts; The Ekman Spiral

It can be observed that the wind speed direction changes from the ground to the top of the boundary layer. Shifts with increasing height are called veering if the wind turns clockwise, and backing if the wind turns counterclockwise.

In the free atmosphere, where the wind is parallel to the isobars, wind direction shifts are caused by the frictional effects of the ground and by the pressure patterns. In this study we are considering a simple model for which we do not need to know the pressure pattern; therefore we will consider only the frictional effects.

In the boundary layer the wind generally turns clockwise (veering); the angle between the wind speed at 3000 feet and the speed near the ground rarely exceeds 35°. The veering is extremely variable, making any quantitative investigation difficult.

The first theoretical study of wind veering was the Ekman-Åberklom model, better known as the Ekman spiral. The derivation of this model is very simple: we write the equations of movement for a laminar horizontal flow in neutral (adiabatic) conditions. Furthermore, isobars are supposed to be straight, parallel and constant with altitude; viscosity and density are also supposed constant with altitude.

In our case, gradient wind and geostrophic wind are the same (see

2.3.1). Their components with respect to the surface wind direction (x axis) are:

$$V_G \cos \alpha_0 = -\frac{1}{\rho f} \frac{\partial \bar{p}}{\partial y} \tag{2.34}$$

$$V_G \sin \alpha_0 = \frac{1}{\rho f} \frac{\partial \bar{p}}{\partial y} \tag{2.35}$$

α_0 is the angle between the surface wind and the geostrophic wind.

Boussinesq equations (Eq. 2.1) yield:

$$-f (\bar{v} - V_G \sin \alpha_0) = \frac{d\tau_x}{dz}$$

$$f (\bar{u} - V_G \cos \alpha_0) = \frac{d\tau_y}{dz}$$

In this case (laminar flow) the shear stress components are given by equation 2.12:

$$\tau_x = \rho_0 \nu \frac{\partial \bar{u}}{\partial z}$$

$$\tau_y = \rho_0 \nu \frac{\partial \bar{v}}{\partial z}$$

Then we have the following differential equations:

$$\frac{\partial^2 \bar{u}}{\partial z^2} + \frac{f}{\rho_0 \nu} \bar{v} = \frac{f}{\rho_0 \nu} V_G \sin \alpha_0$$

$$\frac{f}{\rho_0 \nu} \bar{u} - \frac{\partial^2 \bar{v}}{\partial z^2} = - \frac{f}{\rho_0 \nu} V_G \cos \alpha_0$$

The solution of which is:

$$\bar{u} = V_G (1 - e^{az} \cos az) \tag{2.36}$$

$$\bar{v} = V_G e^{-az} \sin az \qquad (2.37)$$

where $a = \frac{f}{2\rho_0 \nu}$

Sketches of Ekman wind profile and Ekman spiral are plotted in Figures 2.6 and 2.7 respectively. It can be seen that Ekman spiral gives wind shifts of 45°. This is the first shortcoming of this model; rotations greater than 35° are very seldom. This model, valid through the whole boundary layer, should be considered more as a qualitative description than as a quantitative description. In fact the Ekman's profile is unstable and therefore never encountered.

The Ekman spiral can also be considered as a means to compute the height of the boundary layer. For latitudes near to 45° we get a thickness of about 3500 feet which is a good approximation of "average" conditions. However, it should be pointed out that the boundary layer would be infinite at the equator, which is of course not realistic.

Many studies tried to get rid of the main shortcoming of the Ekman spiral: the 45 degrees rotation. Unfortunately many works just try to find a good wind profile or coefficient of turbulence law as an input in Boussinesq equations to get an angle inferior to 45°, which is not difficult! However, some models are derived much more seriously. The problem is that they involve some theories which are well beyond the scope of that study. (See for instance Tennekes, 1972 or Estoque, 1972 for such models.) It is also possible to ex-

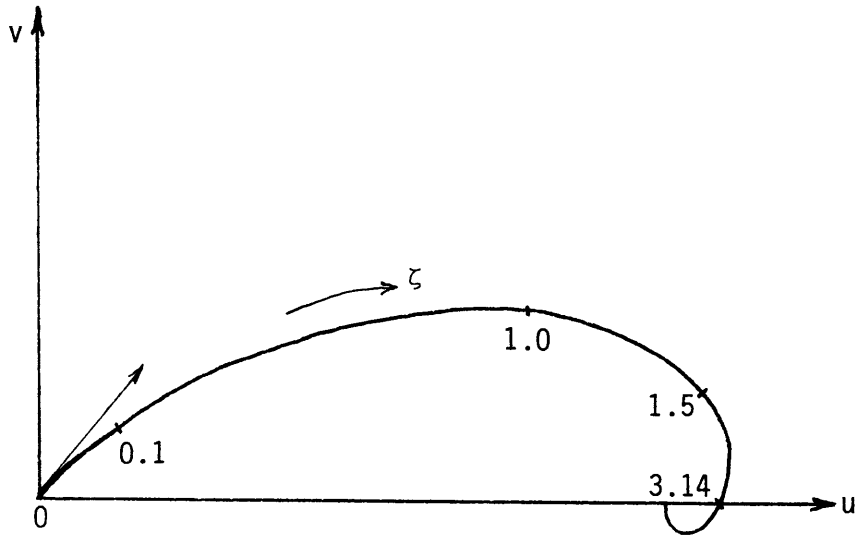

Figure 2.6: Ekman Spiral

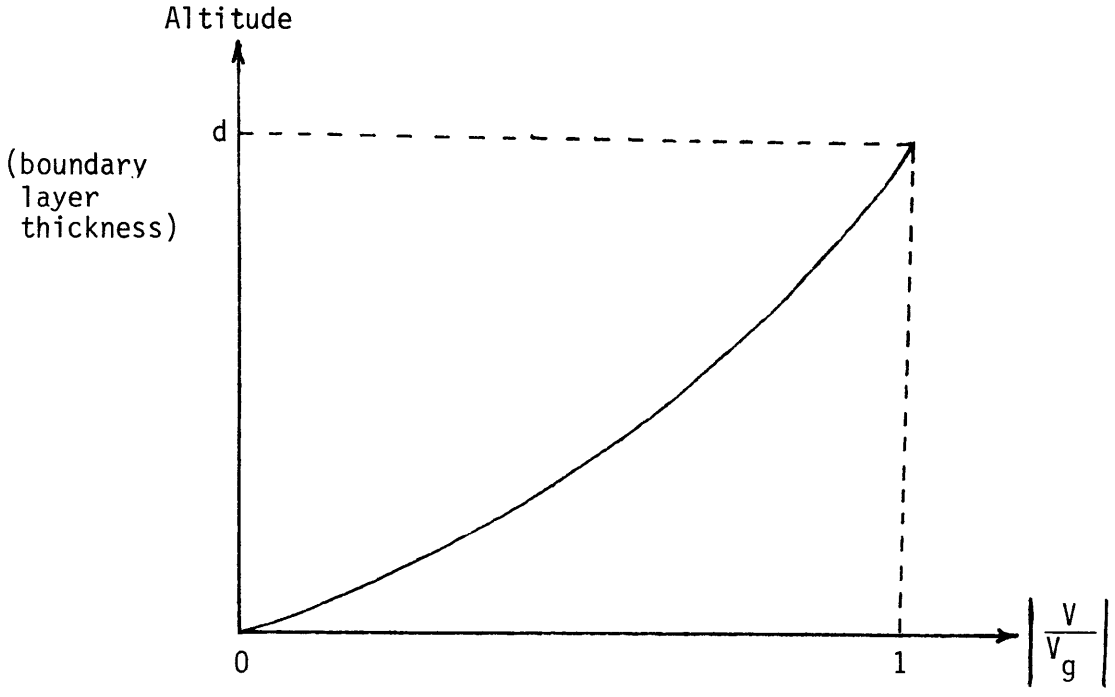

Figure 2.7: Ekman Profile

trapolate all the models of the surface layer. So, we see that the description of wind veering in the boundary layer does not seem to be solved. All the models are valid only in restrictive conditions and are generally very empirical reflecting the important scatter of data in the observations.

2.4 Wind in the Free Atmosphere (Below 10,000 feet)

2.4.1 Geostrophic Wind, Gradient Wind

In the free atmosphere there are at least two causes for wind: Coriolis forces and pressure gradients. In the free atmosphere air particles move with relatively constant direction and speed. Therefore there is a balance between the pressure gradient forces and the Coriolis forces. Moreover, the resulting wind velocity, the geostrophic wind, must blow parallel to the isobars since the gradient force and the Coriolis force are perpendicular to these isobars.

The balance between forces yields the velocity of the geostrophic wind:

$$V_{G_e} = - \frac{1}{f\rho} \frac{\partial p}{\partial n} \tag{2.38}$$

in which n is the oriented normal to the flow with n increasing to the left of the direction of motion. When the isobars are curved, the centripetal force should be considered to balance the forces. The balance between the pressure gradient, the Coriolis force and the centripetal force yields the gradient wind V_{G_r}.

We must make the distinction between cyclonic (low pressure)

and anticyclonic (high pressure) situations. In the Northern hemisphere when the curvature of the path is counterclockwise (cyclonic) the centripetal acceleration is to the left of the direction of motion, as is the pressure gradient force. In anticyclonic situations (clockwise) the centripetal acceleration is to the right of the direction of the flow. Applying once again the Boussinesq equations (Eq. 2.1) we get after some transformations (polar coordinates):

$$V_{G_r} = -\tfrac{1}{2} f r \pm \sqrt{\frac{f^2 r^2}{4} + \frac{r}{\rho}\frac{\partial p}{\partial r}} \qquad (2.39)$$

(r is the radius of the isobar)

A positive value of V_{G_r} corresponds to counterclockwise motion (cyclonic in the Northern hemisphere) and a negative value to clockwise motion (anticyclonic in the Northern hemisphere).

Gradient wind and geostrophic wind may differ significantly, especially in hurricanes: the case when the Coriolis forces are negligible is called the cyclostrophic wind. In this study we will only treat the case of parallel isobars which means that gradient wind and geostrophic wind are equal. We will also neglect all the other effects as thermal winds, or the winds caused by non-horizontal isobars.

2.4.2 Variation of Wind with Altitude

In perfect conditions (straight and horizontal isobars, no horizontal temperature gradient, pressure gradient independent of altitude) the wind speed would be constant in the free atmosphere. Practically, the wind speed and direction are not constant in the free atmosphere.

However, a model describing these variations should take into account the particularities of pressure and temperature patterns.

Since we want a simple model, the only way to solve our problem is to use experimental data. Concerning the wind direction shifts, it is observed that in the Northern hemisphere southerly surface winds continue to veer with altitude above the boundary layer, while northerly winds show backing. Southerly surface winds show an average veering of 0.7 deg/100 feet and northerly surface winds an average backing of 0.7 deg/100 feet between 3000 feet and 10,000 feet at a latitude of about 45° North. This latitude is chosen because most of the American and European airports are approximately at this latitude.

The wind direction shifts are also affected by the time, in the day and in the year, and by thermal conditions, but since the variations due to these factors are on the average less important than the surface wind speed direction, they will be neglected.

The wind speed continues to increase up to an altitude of about 35,000 feet. The wind shear can be considered constant from 3000 feet to 30,000 feet. Since the data on wind shears are rather scarce, we will just give a value of 0.01 S^{-1} found from AN/GMD-2 soundings at Hanscom Field, Massachusetts (3 April 1957) which will be considered as "average" without any justification.

2.5 Wind Model Selection

2.5.1 Simulation Requirements

We need to have a wind profile from 10,000 feet to the ground.

Since the main purpose of this work is to study the influence of disturbances on aircraft scheduling, the accent should be on the wind shear rather than on the wind direction. The model must be implemented on a real time computer but the wind profile can be derived off-line once the local atmospheric data (wind speed, stability,...) are known. However, an off-line computation requests a large memory storage.

The models chosen must represent a wide variety of cases in order to study efficiently the effect of local conditions. Therefore, the models will be chosen according to their good approximation of wind shear and their ability to cover most of the cases encountered in real approaches without worrying too much about computation speed.

2.5.2 Surface Layer

Many data and theoretical studies are available for the surface layer; the main source of data is tower observations. The methods and results can be found in Priestley 1959, Lumley and Panofsky 1964, Monin and Yaglom 1971, Panofsky 1973, Busch 1973, and Dyer 1974.

It has been found that the logarithmic profile and the power law are excellent approximations in the case of neutral stratification. However, since we are looking for a model valid for wide conditions of stability, they will be rejected.

The log-linear profile and the extensions of this profile (exponential-logarithmic, Deacon, Keyps, ...) seem to have serious shortcomings at least for a part of the stability range usually encountered. The method which seems to fit best is the direct application of Monin-

Obukhov similarity theory, that is, the use of universal functions (Eq. 2.19, 2.20).

The best results at this date seem to have been obtained during the 1968 campaign of the Air Force Cambridge Research Laboratories (AFCRL) (Businger et al. 1971, Haugen et al. 1971, Businger 1973). A model using the similarity theory (2.2.3) was developed by fitting universal functions of equations 2.19 and 2.20 with experimental data.

However, this model is only valid for $-2.5 < \zeta < 2$, therefore another model should be chosen to cover a broader range of stabilities. The best solution to solve this problem is to combine several models: logarithmic profile (Eq. 2.25) for neutral stability, Keyps interpolation (Eq. 2.30) for instability, log-linear profile (Eq. 2.27) for moderate stability and an extension of it (Webb, 1970) for strong stability.

The validity of the previous profiles is about from the ground to 300 feet; thus, for a rough approximation of arrival times at an airport, it would be better (faster and cheaper) to use a less sophisticated model such that the power law could be the same as that for the boundary layer. The only difference between the boundary layer and the surface layer would be, in this case, a constant wind direction for the surface layer.

To conclude this study on wind profiles in the boundary layer we will make the following recommendations:

- Accurate landing simulation (autoland tests, ...):
    - Near neutral conditions: AFCRL model
    - Far from neutral conditions: composite model

- Long approach simulations without emphasis on final approach (workload or safety evaluation, ...):
    - Power law model or logarithmic profile with constant speed direction.

2.5.3 Boundary Layer

For the boundary layer we have a choice between Ekman spiral, its extensions, the power law, a constant wind shear, a more sophisticated model with universal functions (similarity law), or extrapolations of surface layer models.

The Ekman spiral seems only descriptive and gives only a rough approximation of the wind profile. Therefore we shall eliminate this model. The model which would probably yield the best results is the general model with the universal functions of Monin-Obukhov similarity law.

However, these universal functions have not yet been determined because of the lack of data. (Some indications on these functions are given in Clarke and Hess 1974, Melgarejo and Deardorff 1974.)

The next best model is the extrapolation of the surface layer models. Unfortunately the extensions of the models selected in 2.4.2 have no analytical expression for instability conditions, in which case the profile must be computed by numerical integration. Most models give only the profile of the module of the velocity. A law for the variation of wind direction must be selected. It has been found experimentally that the sine of the angle of deviation with respect to geostrophic

wind is uniformly distributed between the top of the surface layer and the top of the boundary layer.

The shift angle of the wind at the top of the surface layer (α_{SL}) has a value which can be approximated by:

$$\sin \alpha_{SL} = -10.7 \frac{u_{*0}}{V_g} \left(1 - \frac{z_{ref}\, z_{SL}}{z_{BL}}\right) \qquad (2.40)$$

z_{SL} is the thickness of the surface layer and z_{BL} is the thickness of the boundary layer. This thickness, z_{BL}, is extremely variable with time; however a very rough approximation is given by (Matveev, 1965):

$$z_{BL} = \frac{246\, \bar{u}_{ref}}{|\sin \phi| \log \frac{z_0 + z_{ref}}{z_0}} \qquad (2.41)$$

ϕ is the latitude of the airport (44° 22' N for Boston).

We will make the following recommendations for the choice of the model in the boundary layer according to the simulation needs:

- Accurate simulation of approach (study of automatic landing, for instance) or study of the influence of stability conditions: extrapolation of the composite model of the surface layer.
- Rough simulation (reproduction of "average" phenomena):
  - Power law (Eq. 2.33):

$$\bar{u} = \bar{u}_{ref} \left(\frac{z}{z_{ref}}\right)^p$$

A nominal value of p = 0.18 will be taken. However, it is possible to

vary p in order to get a good representation of the wind shear for different stability conditions.

Over flat land p is approximately normally distributed with a mean of 0.18 and a variance of 0.15 (Hemesath et al. 1974). For both models the thickness of the boundary layer is given by equation 2.41 and the repartition of the shift angle of windshift by extrapolating 2.40 linearly in sin α. This linear extrapolation yields:

$$\sin \alpha = \sin \alpha_{SL} \frac{z_{BL} - z}{z_{BL} - z_{SL}}$$

The simulation of the wind mean will be examined in more detail in 4.4.1.

2.5.4 Free Atmosphere

In the free atmosphere there are no satisfying models available, therefore we will choose a very descriptive and empirical one.

It will be assumed that the wind shear is constant between the top of the surface layer and 10,000 feet. Except if the experimenter wants to fix the value of wind shear, a value of 0.01 S^{-1} will be chosen.

The veering chosen will also be constant: 0.7 deg/100 feet for southerly surface winds and -0.7 deg/100 feet for northerly surface winds. The value of veering for any other surface wind direction will be computed by linear interpolation between these two values.

CHAPTER III

TURBULENCE MODEL

3.1 Introduction

3.1.1 The Necessity of a Turbulence Model

The definition of turbulence was given in 2.1: it corresponds to frequencies higher than the observed gap in the power spectrum of wind velocity.

Most studies on the influence of turbulence on aircraft are primarily concerned with high frequencies. These high frequencies are of the greatest importance for structural design, pilot workload evaluation, automatic pilot design and certification, safety problems, etc.

Turbulence is a zero mean process and therefore the high frequencies have no significant effect on navigation. However, the low frequencies of turbulence must not be neglected; their influence on speed estimation, and consequently time control, must be estimated.

For this reason, a model must be built for the low frequency components of the turbulence. But since the majority of models are valid on the whole range of turbulence (of 3.2), we will develop a model giving all the spectrum. If we wanted to study the influence of a particular range of components, the output of the model should be filtered. In fact, such a study would not be very interesting; we just want to simulate (for evaluation) the influence of turbulence on time accuracy.

We do not care at all to know that the main effect is caused by low frequency components if it does not simplify the simulation.

The models developed here will be very simple in order to be implemented on a real time computer for flight simulation. Consequently, since it is neither a model for atmospheric research nor for fluid dynamics research, the theoretical approach of modeling will be very short and simplified.

This may appear in opposition with the study of wind profiles (Chapter II) which described most of the models now available and gave at least some indications on their derivations.

There are essentially two reasons to explain this different attitude. First, the studies of turbulent flows are incredibly numerous and it is not even useful to give a bibliography on this matter; it is quite easy to get excellent references elsewhere. Second, and more important, a theoretical approach of turbulence is well beyond the scope of this study and is of little interest in the selection of a model. On the contrary, in the wind profile models the theory was simpler and the simplification had a physical interpretation allowing us to define the limitations of the models in many cases.

3.1.2 Some Theoretical Considerations

(For more details, see the excellent books of Monin and Yaglom, 1971 and 1975.)

The equations of movement are the six equations described in 2.2.2: conservation of momentum (Navier Stokes, 3 equations), conservation of mass (continuity equation), energy (entropy equation), and equation of

state. But in contradiction with 2.2.2, the molecular contributions to the momentum and heat fluxes cannot be neglected.

Furthermore, as pointed out in 2.2, there is a "closure problem": when averaging at the "laboratory scale" (2.2.2), we get more unknowns than equations. These supplementary unknowns are the correlations between variables.

In order to solve this problem and to simplify the equations, some hypotheses are usually made. The statistical process describing the turbulence is supposed stationary, homogeneous, and ergodic (time average equivalent to space average, itself equivalent to ensemble average).

Another hypothesis is often made: the Taylor's hypothesis (1938). According to this hypothesis the turbulence can be considered to be frozen in space (Monin and Yaglom, 1975). This simplification can be justified by the fact that the aircraft flies at a speed much higher than turbulent velocities or their rates of change. Therefore, for a time displacement τ (assuming stationarity) and a space displacement $\vec{\xi}$ the correlation function of the process is given by:

$$R_{ij}(\vec{\xi},\tau) = f_1(\vec{\xi})$$

In all the models considered, we will suppose all these hypotheses valid; otherwise, a simulation, or worse, a real-time simulation, is almost impossible.

In the turbulence, two sorts of phenomena take place:

- Mechanical and thermal production of turbulent energy
- Dissipation (by wind shear).

The first phenomenon occurs at long wavelengths while the second is produced at short wavelengths, as it is observed in the turbulence spectrum. Between these two wavelengths there is approximately no modification of energy, it is simply transported from long wavelengths (corresponding to large eddies) to shorter wavelengths (small eddies) by inertial forces. This domain in the wavelengths of turbulence is called the inertial subrange (see Gifford, 1959).

Practically, large eddies break into smaller and smaller eddies until they disappear by viscosity. This physical view of turbulence has an interesting theoretical consequence, the so-called "five-thirds law" (sometimes called the -5/3 law) (MacCready 1962, Obukhov 1962, Syono and Gambo 1952). This law is derived from the hypotheses of Kolmogorov, who proved an equivalent law (the two-thirds law). Obukhov first proved the five-thirds law, which assumes that the spectral energy varies with $\Omega^{-5/3}$ (Ω : spatial frequency). This law is remarkably confirmed by observations by the LO-LOCAT study of the Air Force Flight Dynamics Laboratory.

3.1.3 Procedure for Model Selection

Given these hypotheses (stationarity, homogeneity, ergodicity, Taylor's hypothesis, and the -5/3 law), many models were developed. We will not deal with the details of the derivations but we will examine only the more simple ones which are usable for simulation purposes and which are in agreement with the observations, especially at low frequencies. As usual, a distinction will be made between the differ-

ent layers: surface layer, boundary layer and free atmosphere.

The models examined, as noted before, will reproduce the whole frequency spectrum. Since this is done at no extra cost, there are only advantages. The low frequencies will allow us to study the influence of simulation on timing, and the high frequencies will reproduce a workload for the pilot. Furthermore, these high frequencies do not have the same effects on different aircraft, thus they will be very useful in the simulations where longitudinal or lateral separations are required. This is, for instance, the case for four-dimension simulations during the approach or approach on two close runways.

3.2 Turbulence in the Boundary Layer

3.2.1 Experimental Data

In the context of turbulence, stability and instability are often mentioned, but they do not have the same meaning as in the context of mean wind. It has been observed that turbulence appears for a Richardson's number R_i lower than a certain value, called critical Richardson's number. Its value is approximately 0.25. Therefore, situations in which R_i is superior to the critical Richardson's number are called stable (no turbulence), whereas in the other cases, the situations are qualified as unstable. We recall that generally (e.g. mean wind) stable is understood as $R_i > 0$ and unstable as $R_i < 0$.

It has been observed that the spectral density $S(\Omega)$ is proportional to Ω^{-n} ($n = 5/3$ for the minus five thirds law). As cited before, the

best investigation was probably the LO-LOCAT (Low Low Altitude Critical Atmospheric Turbulence) Project: approximately 200,000 statute miles flown. On the average the exponent n increases with altitude for the long wavelength region of horizontal turbulence (Vinnichenko et al., 1973). This phenomenon is due to the increase of stability with altitude. However, n=5/3 can be considered as an excellent approximation. For the vertical component, the minus five thirds law is also an excellent approximation up to at least 1 km. Above this altitude, n increases slightly.

Comparisons were also made on the variances σ^2_u and σ^2_w of the horizontal and vertical components of turbulence respectively. The value of σ_u/σ_w is very controversial, but it seems that it is greater than one and decreasing with altitude (Chalk et al., 1969; Pitchard, 1966). This ratio also has daily and yearly variations which will not be taken into account here.

Several models were developed based partly on theoretical considerations and partly on observations. In this study we will examine only the more classical ones, which implies that all the mechanisms of model selection are not presented here.

3.2.2 Von Kármán Spectrum

The approach of Von Kármán was to try to find an analytical expression for the energy spectrum $E(\Omega)$. He proposed the following form:

$$E(\Omega) = \frac{A\sigma_g^2 \, (\Omega/\Omega_0)^4}{[1 + (\Omega/\Omega_0)^2]^{17/6}} \qquad (3.1)$$

Ω is the spatial frequency:

$$\Omega = |\vec{\Omega}| = |\Omega_1 \vec{i} + \Omega_2 \vec{j} + \Omega_3 \vec{k}|$$

Numerically:

$$E(\Omega) = \frac{55}{9\Pi} \sigma_g^2 L_T \frac{(1.339\ L_T\ \Omega)^4}{[1 + (1.339\ L\ \Omega)^2]^{17/6}} \qquad (3.2)$$

in which L_T is the scale of the turbulence and σ_g^2 the variance. Their values will be discussed in 3.2.6.

From this relation it is easy to derive the power spectra in the isotropic case:

Longitudinal power spectrum (one dimensional):

$$\Phi_{pp}(\Omega_1) = \frac{\sigma_g^2 L_T}{\Pi} [1 + (1.339\ L_T\ \Omega_1)^2]^{-5/6} \qquad (3.3)$$

Transversal power spectrum (one dimensional):

$$\Phi_{NN}(\Omega_1) = \frac{\sigma_g^2\ L_T}{2\Pi} \frac{1 + 8/3\ (1.339\ L_T\ \Omega_1)^2}{[1 + (1.339\ L_T\ \Omega_1)^2]^{11/6}} \qquad (3.4)$$

We notice that the Von Kármán spectrum satisfies asymptotically the minus five thirds law. According to the LO-LOCAT measurements, this model fits low altitude turbulence spectrum fairly closely up to wavelengths of 20 km.

3.2.3 Dryden Spectrum

The approach of Dryden is different: he fitted the correlation function of the turbulence with an equation. More precisely, he

assumed that the longitudinal correlation function was:

$$f(\xi) = \exp\ (-\xi/L_T)$$

From this function, the derivation of the other statistical characteristics is easy in the isotropic case:

Energy spectrum:

$$E(\Omega) = \frac{8\ \sigma_g^{\ 2}}{\Pi}\ \frac{(L_T\ \Omega)^4}{[1 + (L_T\ \Omega)^2]^3} \tag{3.5}$$

Longitudinal power spectrum (one dimensional):

$$\Phi_{pp}(\Omega_1) = \frac{\sigma_g^{\ 2}\ L_T}{\Pi}\ [1 + (L_T\ \Omega_1)^2]^{-1} \tag{3.6}$$

Transversal power spectrum (one dimensional):

$$\Phi_{NN}(\Omega_1) = \frac{\sigma_g^{\ 2}\ L}{2\Pi}\ \frac{1 + 3\ (L_T\ \Omega_1)^2}{[1 + (L_T\ \Omega)^2]^2} \tag{3.7}$$

It appears that the Dryden spectrum has an asymptotic comportment in Ω^{-2}. In fact, Dryden and Von Kármán spectra are particular cases of the model given by the following power spectra:

$$\Phi_{pp}\ (\Omega_1) = \frac{\sigma_g^{\ 2}\ L_T}{\Pi}\ [1 + a^2\Omega_1^2]^{-n-\frac{1}{2}} \tag{3.8}$$

$$\Phi_{NN}\ (\Omega_1) = \frac{\sigma_g^{\ 2}\ L_T}{2\Pi}\ \frac{1 + 2a^2\Omega_1^2\ (n+1)}{(1 + a^2\Omega_1^2)^{n+3/2}} \tag{3.9}$$

Dryden model: $n = 1/2$; $a = L_T$

Von Kármán model: $n = 1/3$; $a = 1.339\ L_T$

3.2.4 Other models, Gaussian and non-Gaussian models

Some other spectrum models which are of comparable complexity are available; for instance, those of Lappe, Lumley-Panofsky, and Zbrozek. However, these models have nothing new and thus will not be treated here.

Of more importance is the distinction between Gaussian and non-Gaussian models. Dryden and Von Kármán models are usually used to shape a Gaussian white noise. However, this method does not reproduce the patchy nature of turbulence which is commonly observed. In order to reproduce this particular structure of observed turbulence, new models were developed. The most common merely consist of replacement of the Gaussian white noise by a product of two independent Gaussian processes. The multiplication is applied after filtering.

This method gives better results than with Gaussian inputs. In fact, it is not at all surprising that, with more complexity, the approximation is better, especially if this modification is only empirical!

3.2.5 The Problem of Anisotropy

High altitude turbulence may be considered isotropic. However, at low altitudes, especially in the surface layer, the influence of the ground is important. As a consequence we must make the distinction between horizontal and vertical spectra.

This problem is usually solved in an empirical way. Different scale lengths and variances are used for horizontal and vertical spectra.

This method has been found to fit experimental data quite well. Therefore, we will adopt a scaling length L_H and a variance σ_H^2 for horizontal turbulence and a scaling length L_V and a variance σ_V^2 for vertical turbulence. This method can be used for either Dryden of Von Kármán spectra; scaling length and variance are the same for these two models.

3.2.6 Parameter Estimation

Since our problem is now non-isotropic we have to estimate four parameters:

- L_H and L_V
- σ_H and σ_V

The scaling length L is approximately equal to the height above the surface in neutral or unstable stratification and over a smooth surface. However, this value depends upon the nature of the ground and of thermal conditions and wind shears in a very complex way.

Assuming that turbulence must be isotropic for high frequencies and that, in this case, the minus five thirds law is asymptotically verified, we must have:

$$\lim_{\Omega_1 \to \infty} \left(\frac{\Phi_V}{\Phi_H} \right) = \frac{4}{3}$$

which gives:

$$\frac{\sigma_H^2}{L_H^{2/3}} = \frac{\sigma_V^2}{L_V^{2/3}} \qquad (3.10)$$

The scale lengths selected are derived from Dryden spectrum:

$$\begin{aligned} L_V &= z \qquad \text{for } z \leq 1750 \text{ feet} \\ L_V &= 1750 \qquad \text{for } z \geq 1750 \text{ feet} \end{aligned} \tag{3.11}$$

$$\begin{aligned} L_H &= 145\, z^{\frac{1}{2}} \qquad \text{for } z \leq 1750 \text{ feet} \\ L_H &= 1750 \qquad \text{for } z \geq 1750 \text{ feet} \end{aligned} \tag{3.12}$$

We need only σ_V to determine the variance through equation (3.10). σ_V can be estimated with the help of the similarity theory. It has been shown and observed that in neutral conditions σ_V is approximately given by:

$$\sigma_V = 1.3\, u_* \tag{3.13}$$

u_* was given in Chapter II:

$$u_* = u_{*_0} \left(1 - \frac{z}{z_{BL}} \right) \tag{3.14}$$

The determination of u_{*_0} is made by the means of the wind profile and an observation of the wind at a reference altitude. Although the observations are not very precise, some authors tried to evaluate the effects of non-neutral stability. The turbulence decreases with altitude in stable and neutral conditions. In unstable atmosphere, the variance can sometimes increase with altitude.

These laws of variation are generally very complex and are responsible for a large increase of complexity in a real time simulation,

for an unapparent advantage. However, if the simulated model does not need to be flown by a pilot, such a complex model could be examined in some particular cases.

3.3 Free Atmosphere

By definition, the flow should be laminar in the free atmosphere. However, turbulence is sometimes encountered above the boundary layer. This turbulence may be of two sorts:

- turbulence in clouds or near the clouds: convective turbulence,
- turbulence in clear air: clear air turbulence (CAT).

In fact, below 20,000 feet, clear air turbulence in the free atmosphere is very rare and therefore it will not be modeled here. Turbulence in clouds will not be examined either. It seems that the influence of convective turbulence in the free atmosphere is of little importance in time control. Furthermore, since it is not the most common meteorological situation, the interest of building a special model seems marginal. An easier way to simulate turbulence in the highest layer is to modify artificially the height of the boundary layer and to assume that the turbulence is not too different in the free atmosphere and at the top of the boundary layer.

We must also say that in this study, many phenomena were neglected, in the high frequencies as well as in the low frequencies.

In the very high frequencies (less than 0.01 foot), there appears a turbulence of energy spectrum in Ω^{-7} (Heisenberg). In the low fre-

quencies, we ignored atmospheric tides (periods of 12 and 24 hours) of course, and also Rossby waves (approximately 10 waves per day due to variation of the Coriolis parameter), cyclones (approximately one per day), gravity waves (for example, mountain waves, approximately 10^{-1} per second), and gravity-shear waves (Helmholtz waves). The latter are the most common; they appear in regions of rapid variation in the wind velocity (inversions, fronts, etc.).

We will exclude all these phenomena because they are either in a range of frequency without interest for the flight simulation or because they appear only in some particular conditions.

3.4 Model Selection

As previously pointed out, the best source of data is probably the LO-LOCAT study initiated by the United States Air Force. This study gives observation at altitudes higher than tower altitudes and lower than the general flight observations. It was found that the Von Kármán spectrum was much better than the Dryden spectrum at high frequencies (higher than 10^{-2} cpf). However, at low frequencies these models are equivalent. Since we are interested more particularly in low frequencies, the difference between these models is not important.

Thus, the difference between the Dryden and Von Kármán models is not significant regarding the accuracy of the simulation for time control. However, the Dryden model is much simpler to simulate. The Von Kármán model has non-integer exponents and therefore it is only possible to approximate this model by linear filters. On the contrary,

it is easy to build filters which reproduce exactly the Dryden spectrum.

For these reasons the Dryden model was selected for turbulence in the boundary layer. No model of turbulence is considered in the free atmosphere. However, it is possible to increase artificially the height of the boundary layer. In the simulation selected, the experimenter will have the freedom of assigning a height higher than the "true" boundary layer for the upper limit of turbulence. The turbulence in this supplementary layer will have the same characteristics as the turbulence at the top of the boundary layer.

The choice must also be made between Gaussian and non-Gaussian turbulence. The only difference between these two models is that one is probably more realistic than the other. This could be important in landing simulation or workload evaluation.

Kurkowski et al. (1971) tested three different models on the Ames height control simulator. The models tested were a record of real turbulence (from LO-LOCAT program), a Gaussian model and a non-Gaussian model (a product of two Gaussian processes).

Four test pilots participated in the evaluation. The pilots were not able to make a significant distinction between these models. The models were even rated better than the real record in most cases. Then, although a product of Gaussian processes matches real turbulence better than a Gaussian process, no significant preference is shown by the pilots.

In the simulation we will therefore choose a Gaussian white noise as an input of the Dryden spectrum. Therefore, the model selected can be summarized by the equations shown in Figure 3.1.

Figure 3.1: Turbulence Model

Power Spectra:

$$\Phi_u = \Phi_v = \frac{\sigma_H^2 L_H}{\Pi} \frac{1}{1 + (L_H \Omega_1)^2}$$

$$\Phi_w = \frac{\sigma_V^2 L_V}{2\Pi} \frac{1 + 3 (L_H \Omega_1)^2}{[1 + (L_H \Omega_1)^2]^2}$$

Variances:

$$\sigma_v = 1.3\ u_*$$

$$u_* = u_{*_0} \left(1 - \frac{z}{z_{BL}}\right) \qquad u_{*_0} = \frac{k\ \bar{u}_{ref}}{\ell n \frac{z_{ref} + z_0}{z_0}}$$

(z_{BL} is given by the wind profile model.)

$$\sigma_H = \sigma_V \left(\frac{L_H}{L_V}\right)^{1/3}$$

Scaling Lengths:

$L_V = z$ for $z \leq 1750$ feet

$L_V = 1750$ for $z \geq 1750$ feet

$L_H = 145\ z^{\frac{1}{2}}$ for $z \leq 1750$ feet

$L_H = 1750$ for $z \geq 1750$ feet

CHAPTER IV

SIMULATION

4.1 Introduction

We will develop here in some detail the simulation techniques used. The simulation consists of a simulated flight of a Boeing 707-320B observed on a radar scope. The purpose of this study is the simulation of dynamic disturbances, i.e. wind disturbances and radar errors, to analyze their effects on time scheduling in a four-dimension navigation environment.

The simulation of the mean wind profile is straightforward. On the contrary, turbulence and radar error simulations require the use of a white noise generator. The generator chosen was digital to provide very low frequencies.

The white noise generation, the radar and wind models, the problem of transformation of coordinate axes from the wind and aircraft axes to absolute axes, and finally the connection with the aircraft model will be examined in this chapter. The general organization of the simulation is shown in Figure 4.4.

4.2 Noise Generation

4.2.1 Generation of a Uniform Distribution

There are two means of generating random numbers with a digital computer. The first one involves the use of a random number table

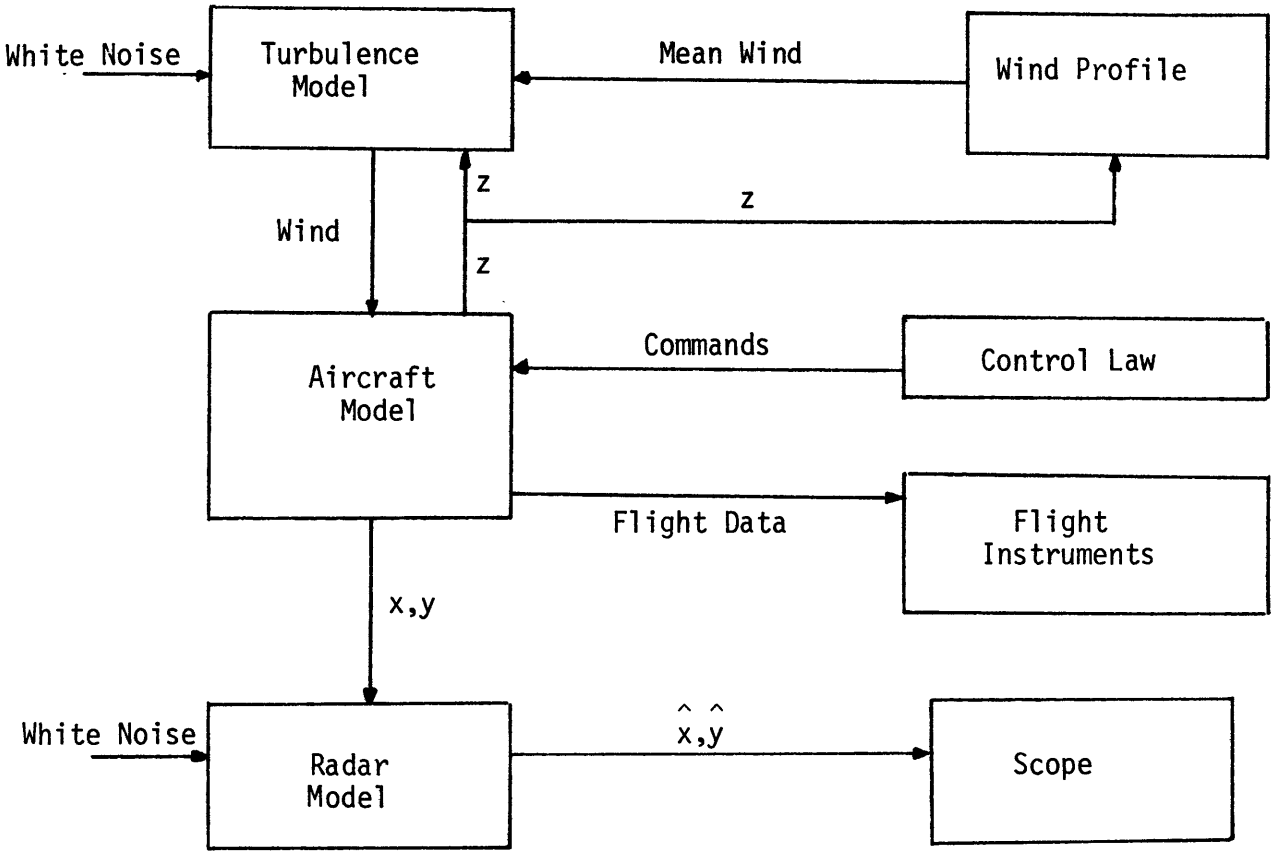

Figure 4.4: Simulation Block Diagram

stored in the computer. The second one is only the generation of pseudo-random sequences by a mathematical process. In fact, there is a third means which consists in using a physical process interfaced with the computer; in our case this technique is not very convenient, therefore the choice is between random number table and mathematical process.

Some very good tables of random numbers are available (Rand Corporation, 1955 for instance). However, they require large storage capacities which are not compatible with many small real time computers.

Therefore we will choose a mathematical process to generate random numbers; these numbers will have a uniform distribution which must be transformed in the desired distribution.

The mathematical process selected is the so-called multiplicative method, also called power residue method or multiplicative congruential method (for more details, see Naylor et al., 1966).

The algorithm used is:

$$X_i = \lambda X_{i-1} \pmod{k}$$

where X_i is the i^{th} random number, and λ and k are two integers. In order to get the largest sequence, that is, the "more random" numbers, λ and k are selected as follows:

$k = 2^n$	where n is number of bits in a computer word (n=30 for the AGT-30)
$\lambda = 8m \pm 3$	where m is a positive integer such that $\lambda \approx 2^{n/2}$

Practically, λX_{i-1} is computed in fixed-point arithmetic, therefore using two words. The lower order n bits give X_i. X_i is then divided

by 2^n to obtain a uniform distribution on the interval [0,1].

The process must be initialized by choosing an odd initial value X_0. With these conditions a period of 2^{n-2} will be obtained (2.7×10^8 for the AGT-30).

4.2.2 Generation of a Gaussian Distribution

Given a uniform distribution on the interval [0,1] we need to generate a given distribution. In general this transformation is done with the aid of the cumulative distribution function:

$$F(x) = \int_{-\infty}^{x} f(\xi)\, d\xi \qquad \text{for a density } f$$

If x has the density f, then $y = F(x)$ is uniformly distributed on [0,1]. Conversely, if y is uniformly distributed on [0,1], $x - F^{-1}(y)$ has the density f. Therefore the mothod consists of obtaining an analytical expression or a numerical approximation for F^{-1}.

For Gaussian distributions, two other methods are commonly used. A direct method: if x_1 and x_2 are two independent random variables uniformly distributed on [0,1], then $y = \sqrt{-2\ \ell n\ x_1}\ \cos 2\Pi x_2$ has a normal distribution N(0,1). The other method uses the central limit theorem: the sum of n independent random variables approaches a Gaussian distribution as n goes to infinity.

If $x_1, x_2, \ldots, x_n$ are n independent uniformly distributed on [0,1] random variables, then

$$x = \sqrt{\frac{12}{n}} \left[\sum_{i=1}^{n} (x_i - \tfrac{1}{2}) \right]$$

is approximately normally distributed ($\bar{x} = 0$, $\overline{x^2} = 1$) for large n. Generally the value n = 12 is used yielding a good approximation up to $3\sigma_x$.

The choice between these methods depends upon the computer employed. The cumulative distribution function method is the fastest but requires a large storage for good accuracy of F^{-1}. The direct method is obviously the most accurate; however, on a computer like the AGT-30 using series to compute the logarithm, cosine and square root functions, it is really very slow.

Consequently the central limit theorem method will be used with 12 points to get a good accuracy . Since it requires twelve random numbers it is moderately fast, but it is a good compromise.

4.2.3 Power Spectrum

We have generated a white noise from a uniform distribution. In fact, this distribution is only pseudo-random; it is periodic. Therefore we must worry about the power spectrum of the white noise obtained.

This distribution has another particularity, it is not stationary, since there is a finite sample time Δt (Figure 4.5). However, for times greater than Δt and smaller than the period T of the random number generator, this process can be considered stationary. Without dealing with the detail of the computations, which are very easy, we give some quantitative results:

- Power spectral density: (Figure 4.5)

$$\Phi_{xx}(\omega) = \frac{\sigma_x^2 \, \Delta t}{2\Pi} \left[\frac{\sin \omega \Delta t/2}{\omega \Delta t/2} \right]^2$$

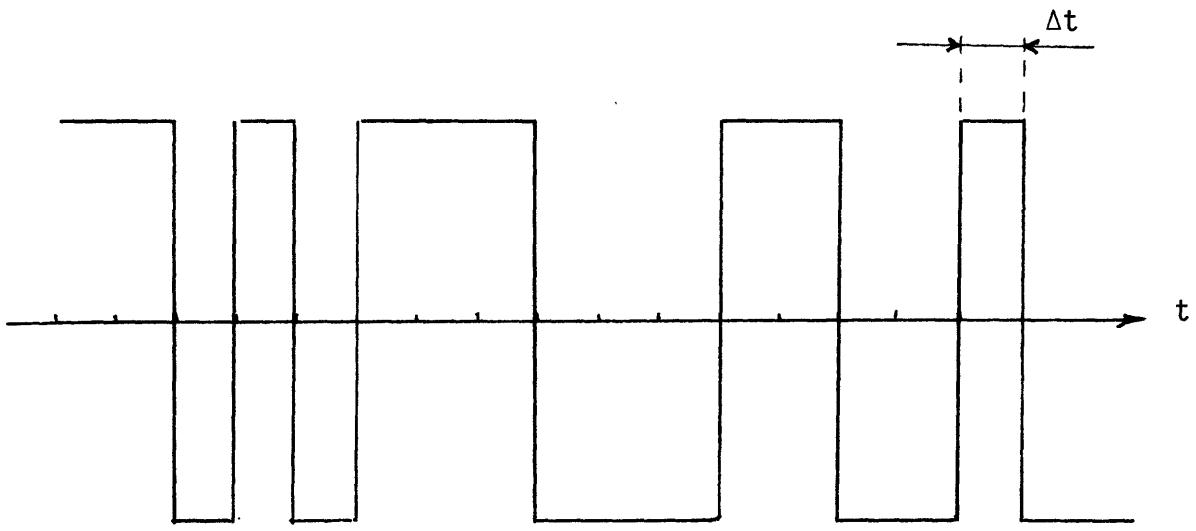

Random Wave

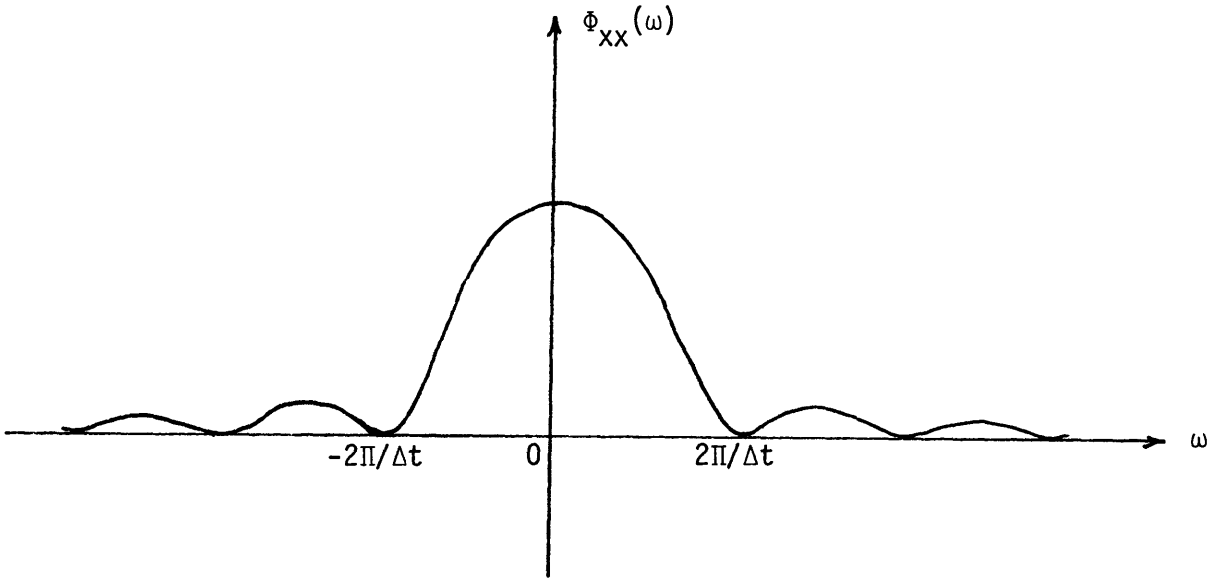

Power Density Spectrum

Figure 4.5: White Noise Spectrum

- The power contribution from each k^{th} multiple of the fundamental frequency (period T) is proportional to

$$\left[\frac{\sin (k \Pi \Delta t/T)}{k \Pi \Delta t/T} \right]^2$$

where k is an integer and can be neglected since $T >> \Delta t$;

- Low frequency gain:

$$\frac{\sigma_x^2 \Delta t}{2\Pi} ;$$

- The noise spectrum is constant at 10 up to approximately $\omega\Delta t = 1.15$;
- The white noise should be adjusted by multiplying it by $\frac{1}{\sigma_x}\sqrt{\frac{2\Pi}{\Delta t}}$.

The white noise generator program, since it is very short and easy, was written in assembly language to minimize the computation time.

4.3 Radar Simulation

Given the coordinates of the aircraft, the radar yields only noisy information. In fact, this noise is induced by fundamental phenomena ahd has a lower bound (see Rihaczek, 1964).

The purpose of this simulation is to reproduce the radar noise. This noise will be supposed to be a Gaussian white noise, independent of the distance from the radar. This assumption seems in good accordance with the reality : the resolution is simulated by Gaussian errors for the bearing and for the range. Standard deviations of 185 feet (range) and 0.25° (bearing) have been selected as typical values for

the airport surveillance radar.

In this model, the radar will not be implemented on the airport. Different radar positions can then be tested. This allows us to investigate the influence of these options particularly on the speed estimation.

We should also notice that although white noise is a stochastic process, we do not have to take particular precautions on the sampling frequency (Nyquist Theorem): the high frequency modes of the aircraft are of course not observable on the radar.

A block diagram of the radar model is shown in Figure 4.6.

4.4 Wind Simulation

4.4.1 Mean Wind and Wind Shear Simulation

The model selected determines the wind profile from the ground up to an altitude of 10,000 feet.

The different inputs of the model are:

- Latitude of the airport, ϕ (if not specified $\phi = 45°$);
- Reference wind: the speed, $\bar{u}_{ref}$, and direction of the wind must be given at a reference altitude, z_{ref} ;
- Wind shear: the wind shear in the boundary layer must be given. It is characterized in the simulation by a value, p of the power in the power law. If this value is not given, the selected power is $p = 0.18$.

From these inputs, the model computes the characteristics of the wind profile. If some parameters such as winds aloft, are known, they are

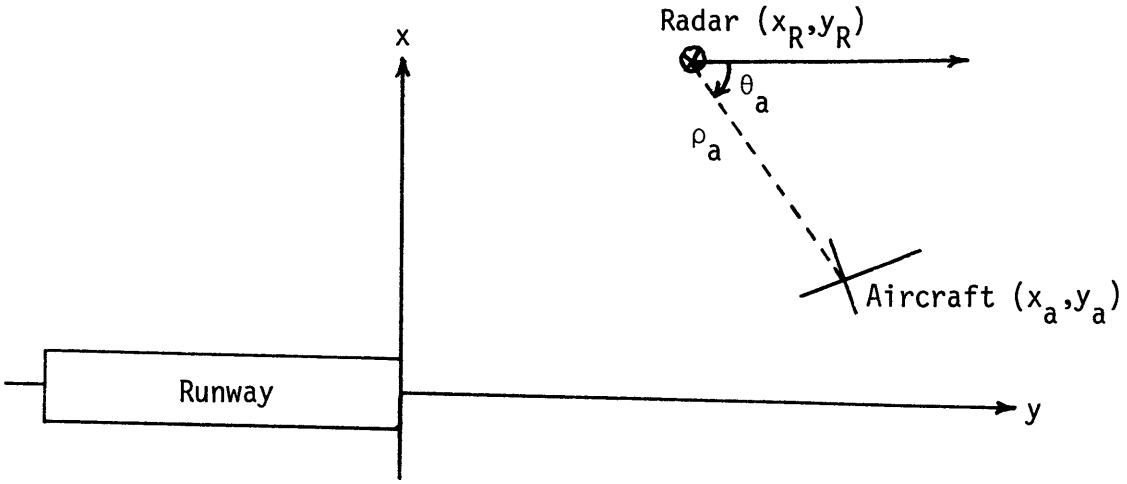

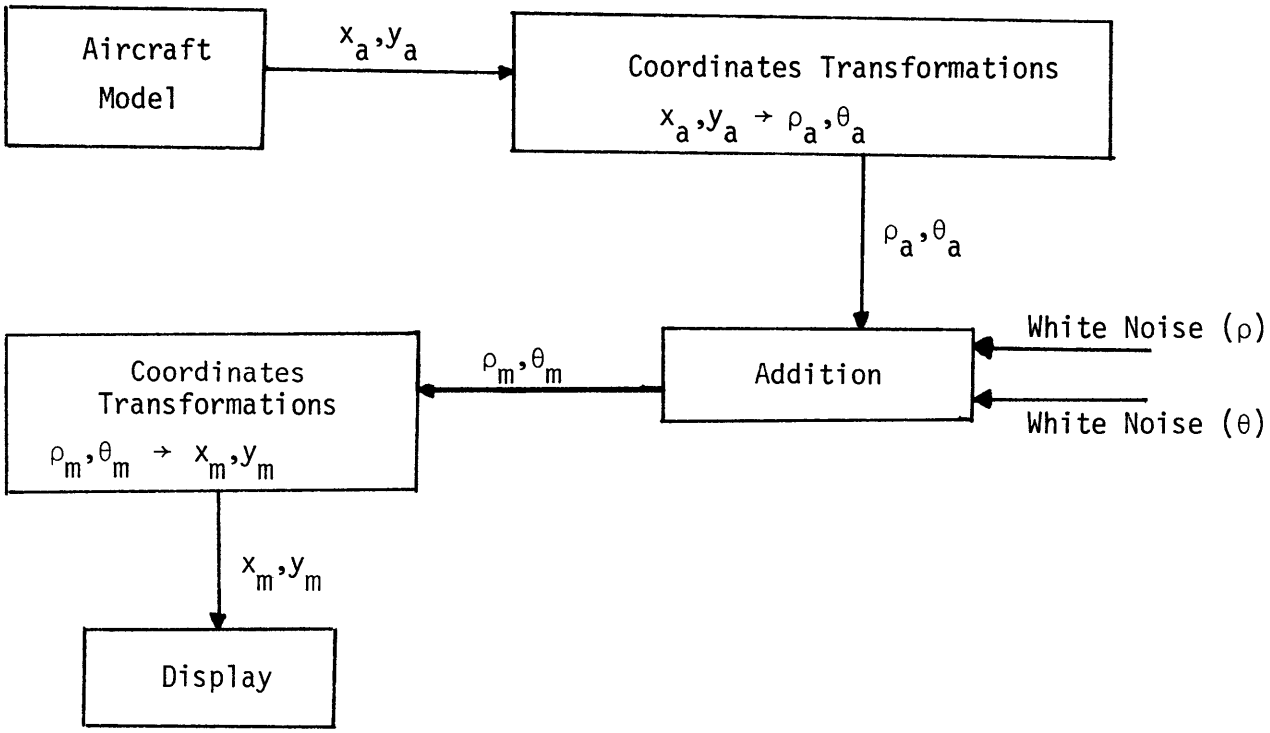

Figure 4.6: Radar Simulation

taken into account and extrapolated by the model. The equations describing the model are the following :

- Boundary layer height:

$$z_{BL} = \frac{24.6\ \bar{u}_{ref}}{|\sin \phi|\ \log \frac{z_0 + z_{ref}}{z_0}}$$

- Roughness length:

$$z_0 = 0.15 \text{ foot}$$

- Wind speed profile:

$$z \leq z_{BL} : \qquad \bar{u} = \bar{u}_{ref}\left(\frac{z}{z_{ref}}\right)^p$$

$$z \geq z_{BL} : \qquad \bar{u} = \bar{u}_{BL} + a(z - z_{BL})$$

($\bar{u}_{BL}$ is the wind at the top of the boundary layer, a is the wind shear in the free atmosphere. A value of 0.01 S^{-1} is taken for a if no observation is known.)

- Shift angle, α (angle from the geostrophic wind);

  - at the top of the surface layer (α_{SL})

$$\sin \alpha_{SL} = -10.7 \frac{u_{*_0}}{\bar{u}_{BL}} \left(1 - \frac{z_{ref} z_{SL}}{z_{BL}}\right)$$

$$z_{SL} = 300 \text{ feet}$$

$$u_{*_0} = \frac{k\ \bar{u}_{ref}}{\ell n\left(\frac{z_{ref}+z_0}{z_0}\right)}$$

with k = 0.35 (Von Kármán constant)

z_0 = 0.15 ft. (Roughness length)

- in the boundary layer $z_{SL} \leq z \leq z_{BL}$:

$$\sin \alpha = \sin \alpha_{SL} \frac{z_{BL} - z}{z_{BL} - z_{SL}}$$

- in the free atmosphere $z \geq z_{BL}$:

$$\alpha = -\left(2b \frac{|180 - D_o|}{180} - b \right) (z - z_{BL})$$

D_o is the direction of the wind near the ground

(180° for southerly wind, for instance)

b is the rate of veering chosen at 0.7 deg/100 feet.

A block diagram of the wind simulation is shown in Figure 4.7.

4.4.2 Turbulence Simulation

The model describes the turbulence in the whole boundary layer, including the surface layer. The turbulence is generated by filtering a Gaussian white noise. For each component, the white noise must have a variance equal to the variance of the turbulence. In fact, since this variance is only a multiplicative factor, it is possible to model it anywhere in the simulation. This allows us to use a standard white noise of variance for all the Gaussian processes.

The filters must be built in order to shape the output spectra, so that they match the Dryden spectra:

$$\Phi_u = \Phi_v = \frac{\sigma_H^2 L_H}{\Pi} \frac{1}{1 + (L_H \Omega_1)^2}$$

$$\Phi_w = \frac{\sigma_V^2 L_V}{2\Pi} \frac{1 + 3(L_H \Omega_1)^2}{[1 + (L_H \Omega_1)^2]^2}$$

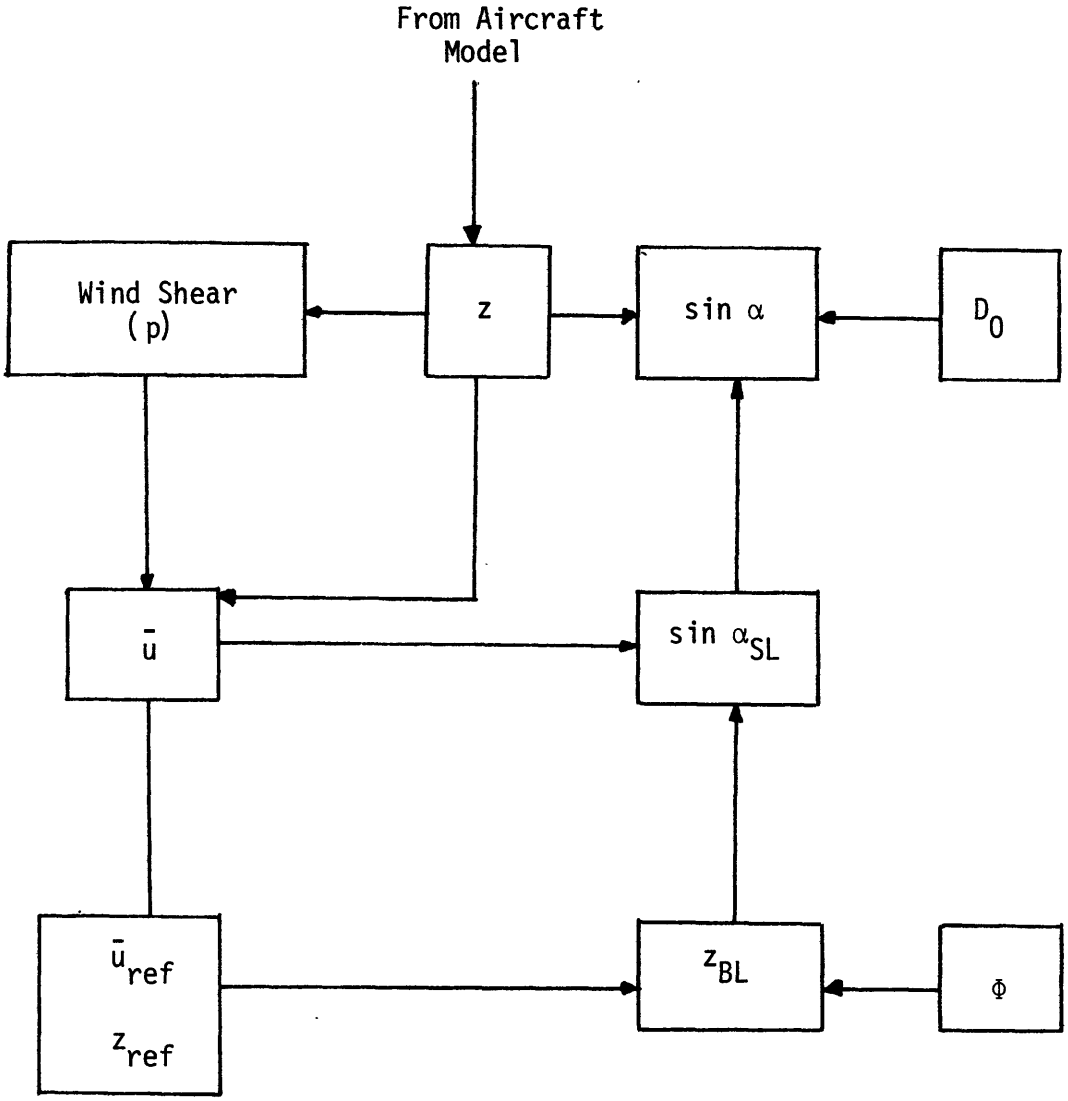

Figure 4.7: Wind Profile Computation

We will suppose the Taylor's hypothesis (3.12) is verified. In this case we have:

$$\Omega_1 = \frac{\omega}{V_A}$$

if V_A is the speed of the aircraft. Then it is quite obvious how to design filters which match the Dryden spectra. If we call Z_u, Z_v, Z_w the transfer functions of these filters and if the variances are included in the filters we have:

$$Z_u(p) = Z_v(p) = \sigma_H \sqrt{\frac{L_H}{\Pi}} \frac{1}{1 + \frac{L_H}{V_A} p}$$

$$Z_w(p) = \sigma_V \sqrt{\frac{L_V}{2\Pi}} \frac{1 + \sqrt{3} \frac{L_V}{V_A} p}{\left(1 + \frac{L_H}{V_A} p\right)^2}$$

The parameters of these equations are given by the following relations:

- Scaling Lengths:

$L_V = z$ for $z \leq 1750$ feet

$L_V = 1750$ for $z \geq 1750$ feet

$L_H = 145 z^{\frac{1}{2}}$ for $z \leq 1750$ feet

$L_H = 1750$ for $z \geq 1750$ feet

- Variances:

$\sigma_V = 1.3\, u_*$

$u_* = u_{*_0} \left(1 - \frac{z}{h_T}\right)$

h_T is the height of the turbulent layer. It is taken equal to the height of the boundary layer, unless otherwise specified in the simulation . u_{*_0} is given by the wind profile model.

$$\sigma_H = \sigma_V \left(\frac{L_H}{L_V} \right)^{1/3}$$

4.4.3 Axis Transformations

In the study of turbulence we never defined precisely in which axes the statistical properties were given. In fact, there is really a problem of axis definition in the study of turbulence.

The power spectra are valid in relative wind axes while the variances are valid in mean wind axis. Furthermore, the problem must be solved in body axes. The transformations of statistical properties from an axis system to another system are theoretically very simple. These computations imply the computation of two 6 x 6 matrices and of their product. Therefore, unless it would be really necessary for the simulation, these transformations will be neglected.

The effect of these transformations is to introduce cospectra especially in the plane u-w. In simulations designed to study the flight qualities of an aircraft, these cospectra should not be neglected. However, the present simulation does not require this accuracy. Therefore we will consider that the projection of the airspeed on the plane of the earth and the projection of x body axis are coincident.

In this case the matrix transformation is merely:

$$\begin{bmatrix} u_B \\ v_B \\ w_B \end{bmatrix} = \begin{bmatrix} \cos\theta & 0 & -\sin\theta \\ \sin\theta\,\sin\Phi & \cos\Phi & \cos\theta\,\sin\Phi \\ \sin\theta\,\cos\Phi & -\sin\Phi & \cos\theta\,\cos\Phi \end{bmatrix} \begin{bmatrix} u_T \\ v_T \\ w_T \end{bmatrix}$$

where u_T, v_T, w_T are the outputs of the filters and u_B, v_B, w_B are the turbulence components in body axes. θ is the pitch angle and Φ the bank angle.

A block diagram of the turbulence simulation is shown in Figure 4.8.

For the mean wind the axis transformations are quite classical:

$$\begin{bmatrix} \bar{u}_{BW} \\ \bar{v}_{BW} \\ \bar{w}_{BW} \end{bmatrix} = \begin{bmatrix} \cos(\Psi - \bar{\Psi}_W)\,\cos\theta \\ \cos(\Psi - \bar{\Psi}_W)\,\sin\theta\,\sin\Phi - \sin(\Psi - \bar{\Psi}_W)\,\cos\Phi \\ \cos(\Psi - \bar{\Psi}_W)\,\sin\theta\,\cos\Phi + \sin(\Psi - \bar{\Psi}_W)\,\sin\Phi \end{bmatrix} \bar{u}$$

in which Ψ is the heading of the aircraft, $\bar{\Psi}_W$ is the heading of the mean wind, and $\bar{u}_{BW}$, $\bar{v}_{BW}$, $\bar{w}_{BW}$ are the components of the mean wind in body axes.

4.5 Aircraft Model

The modeled aircraft is a Boeing 707-320B. The model used is the non-linear model developed by Corley (1974) at M.I.T. In fact, the program selected for the simluation is a derivation of a program

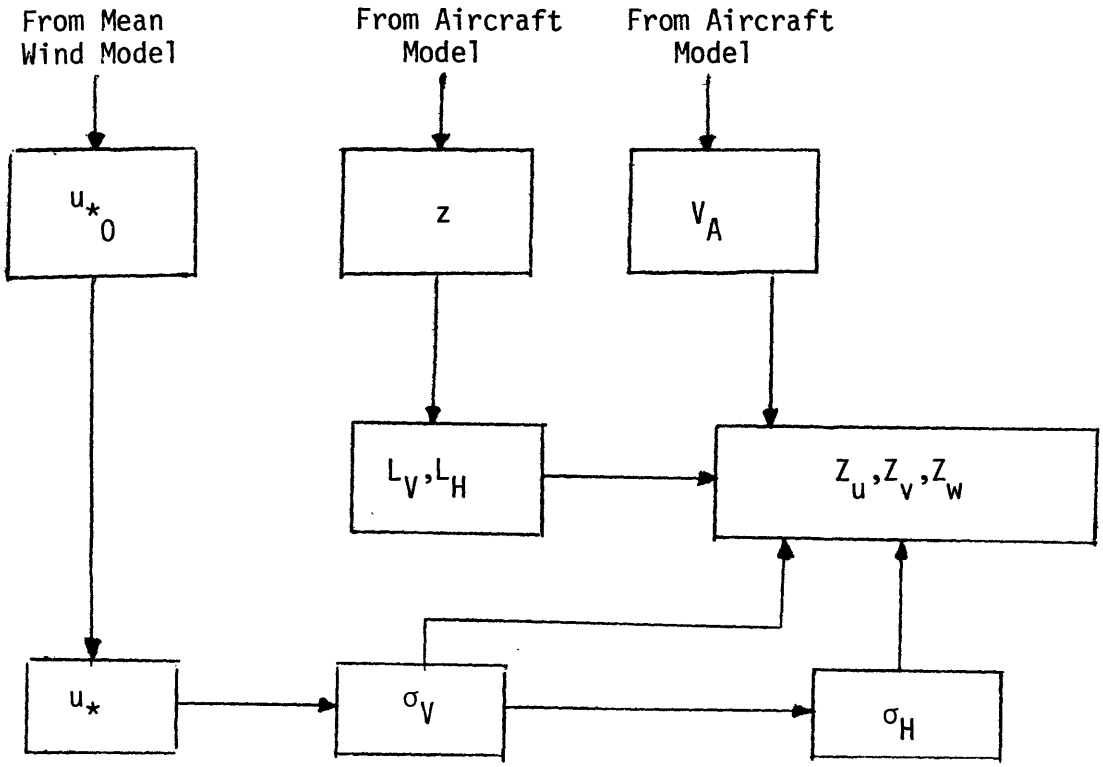

Filter Computation

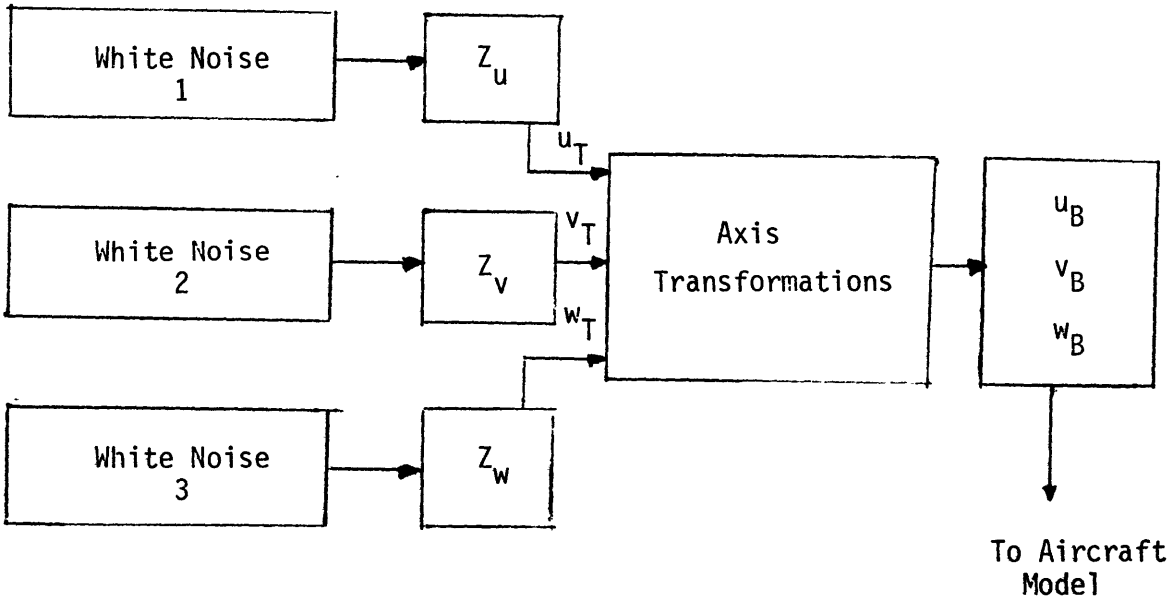

Figure 4.8: Turbulence Simulation

written by Lax (1975) at M.I.T.

The Lax program was selected because it is written in FORTRAN (Corley wrote his program in an assembly language). We think that FORTRAN is obviously not the best language for a real time simulation; ALGOL PIDGIN which is available on the Adage computer would have been preferable, for instance. However, FORTRAN is much better than an assembly language, even for a real time simulation; it is a language very easy to understand by anybody and moreover, programming and maintenance costs are much lower. This last point seems to be forgotten by some researchers. Fortunately there is now an evolution towards high level languages.

Three reference frames were used to describe the motion of the aircraft: wind axes, body axes, and vehicle axes. All these coordinate systems are right handed, orthogonal with the origin at the aircraft center of gravity.

The body axis system has its positive x-axis coincident with the longitudinal axis of the aircraft, positive forward, and its positive y-axis positive towards the right wing. In the wind axis system, the x-axis is coincident with the total aircraft velocity vector and in the vehicle axis the x-y plane is parallel to the surface of the "flat" earth.

The derivations of the equations of movement in these coordinate systems are quite classical, and therefore, will not be developed in detail here.

In this particular simulation the most important range of frequencies

is low frequency, and it is therefore possible to make some simplifications. First, all the effects of the wind will be applied to the center of gravity of the aircraft. In an accurate simulation, study of flight qualities for instance, the repartition of the wind on the aircraft, particularly wind shear and turbulence, should be computed. Furthermore, the wind perturbations will not be considered as an outside perturbation but only as a modification of the wind coordinate system.

It must be pointed out that the model developed here is not valid for the study of the aircraft response to wind gusts. In order to have realistic responses to gusts, special techniques should be used: computation of the repartition of wind on the wings and on the tail, span averaging, etc. In our case, the filters which should be introduced have time constants less than one second and are neglected.

4.6 Simulation Program

The program simulates a flight of an aircraft from 10,000 feet to the ground in the presence of wind disturbances and radar errors. The output of the radar can be used as input in a four dimension navigation controller. The inputs of the program are the location of the radar and the wind at a reference altitude near the ground. If the characteristics of the radar (standard deviations) are not given, typical values are automatically taken (see 4.3).

If the only input of the program for the wind is the surface wind, the wind profile and turbulence characteristics are derived by the pro-

gram from 10,000 feet to the ground. If some other wind characteristics are given by the experimenter (wind shear, winds aloft, turbulence, etc.), these values are taken into account and extrapolated by the program.

The real time simulation computer program is included in the Appendix.

CHAPTER V

CONCLUSIONS AND RECOMMENDATIONS

The objective of this study was to design a wind model and a radar model to estimate the influence of the disturbances affecting strategic navigation. Since our main concern was strategic navigation the emphasis was put on low frequency variations of wind.

There are two means to study the disturbances affecting time and position precision. The first one is to use theoretical models and statistics and to try to determine mathematically the effect of disturbances. The second means is to build a model of disturbances which can be implemented on a flight simulator and to "fly" these models in real time. It is this second option which was chosen in this study.

Concerning the radar model, a very simple model was considered. The free parameters are the radar position and the range and bearing standard deviations. The input of the model is the true position of the aircraft and the output is the noise observation on the controller's scope or on the pilot's scope in the case of the Traffic Situation Display.

Concerning the wind model, a distinction was made between mean wind and turbulence. For each of these models another distinction was made according to altitude: different models were considered for surface layer, boundary layer and free atmosphere. In every case a survey of the different models available for real time simulation was made.

Finally a very simple model was chosen; the principal criteria of selection was speed of computation, given a level of accuracy sufficient for this simulation (low frequency variations of wind).

With these radar and wind models a program of real time simulation was written. In order to interface these models with an aircraft model, several operations were necessary; axis transformations and sampling for instance. The result is a program which can be implemented with many other aircraft models with only a few modifications in the transmission of the parameters. Furthermore, the input of data is conversational and is well adapted to the needs of users. It is also completely independent of the aircraft simulation program and is therefore always available.

Some recommendations should be made for further research in wind modeling for real time simulation. Two aspects must be considered: speed and accuracy. This program was written in FORTRAN which is not very efficient. It would be very interesting (if the wind simulation slows down the aircraft simulation too much) to write the simulation in a more efficient model. However, an assembly language should be avoided; the documentation, maintenance and design of such a program are too difficult and costly.

Another solution could be to use a faster computer; the Adage computer is wonderfully designed for displays, but unfortunately the computation of transcendental functions is slow.

Concerning accuracy we must make the distinction between the wind model itself and its connection with the aircraft model. This study

gives many indications about other more refined models. The mean wind model in the boundary layer is probably too simple. Some other parameters such as stability should be considered if more accuracy is needed.

The connections with the aircraft model can be improved by introducing the side slip angle in the axis transformations. Furthermore for special simulations (evaluation of workload in turbulence, for instance) the distribution of wind on the aircraft should be considered and more care for sampling periods should be taken. It may be necessary in some cases to filter the turbulence before applying it to the aircraft model.

To sum up these recommendations, we can say that some improvements can easily be made in order to use the wind models not only to study the influence of wind on time precision but in most real time flight simulations.

The immediate applications of this program are time precision studies in strategic navigation environment, evaluation of 4-D Navigation algorithms, design and evaluation of 4-D Navigation controllers, evaluation of Traffic Situation Display, evaluation of alarms (Collision Avoidance System, for example), testing of new equipment (RNAV, Inertial navigation, ...), pilot training and testing with respect to time and position accuracy in strategic navigation environment.

The program designed here is a good simulation of turbulence for time accuracy, but is probably not very realistic for the pilot. With a few modifications, as noted before, a similar model could be used for

workload estimation, testing of automatic pilots and pilot training and testing in all phases of the flights.

A refined model of wind could also be used to test much simpler models which could be implemented on board aircraft for in-flight estimation of wind.

APPENDIX

Computer Programs

The programs developed here allow the computation of dynamic disturbances, i.e. wind disturbances and radar errors, as described in Chapter IV - Simulation - . These programs are designed to be "flown" on a flight simulator in real time by pilots.

A precise description of the programs is given here so that it should be easy for future researchers to use or modify them.

The theoretical aspect of the simulation was developed in Chapter IV; the equations were just translated into FORTRAN. Two programs ("INITWIND" and "INITRADAR") initialize the computations for wind and radar; they ask the operator to input the characteristics of wind and radar and perform all the computations that can simplify the real time simulation. This real time simulation of disturbances is performed by the programs "WIND" and "RADAR".

However, these programs require an aircraft model. This aircraft simulation program is just an adaptation of a program written by Lax (1975). The programs of the aircraft simulation are:

- "CONTROL" (Main program) which initializes and controls the simulation;
- "SAMPLE" which samples cockpit controls;
- "BEACONS" which operates Market-Beacons lights;
- "DYNAMICS" which simulates the dynamics of the aircraft;
- "RTOF" which converts data real to fraction for the displays;

- "DIALS" which displays the instrument panel.

These programs will not be examined here; for more details on the original programs (without the option facilities) see Lax's report (1975).

We will now examine the different inputs and outputs of the simulation of disturbances. For the radar simulation the inputs are the coordinates of the radar, the coordinates of the aircraft and the bearing and range standard deviations. The outputs are the noise coordinates of the aircraft.

For the wind simulation the inputs are partially aircraft parameters: altitude, heading, speed, aerodynamic angles, Euler angles; and partially wind parameters: surface wind, wind shear, wind veering, turbulence. The outputs are the components of the aircraft velocity in body axes.

The end of this appendix contains the listings of the programs, a list of the important FORTRAN variables and equations, and a block diagram of the computations so that is should be easy to use or modify the programs.

List of Principal FORTRAN Variables

Radar Program Variables

XM,Y	Aircraft coordinates in miles and feet, respectively
XR,YR	Radar Coordinates in feet
XMMES,YMES	Noise measured coordinates in miles and feet, respectively
SIGBRG,SIGRGE	Bearing and range standard deviations in degrees and feet, respectively

Wind Program Variables

A	Aircraft altitude
PSI	Aircraft heading
VTOT	Module of aircraft airspeed
UVEL,VVEL,WVEL	Aircraft speed components in body axes
CTTET,CFIE,STTET,SFIE	Euler angles: cosines and sines
VW,PSIW	Wind speed and heading
VWREF,PSIWO,ZREF	Module, heading and height of reference wind
ZO	Roughness length
P	Power Law parameter
ZBL,ZSL,ZTURB	Heights of boundary layer and surface layer
VRGFA	Veering factor (free atmosphere)
WS	Wind shear (free atmosphere)
VG,PSIWG	Module and heading of geostrophic wind
ALPSL	Shift angle from the geostrophic wind at the top of the surface layer
U,V,W	Mean wind components in body axes
UT,VT,WT	Turbulence components in body axes

Note: Input units for velocity and angles are knots and degrees respectively. Feet per second and radians are used internally.

Principal FORTRAN Equations

Friction Velocity at the Surface:

$$u_{*_0} = \frac{k\bar{u}_{ref}}{\ell n\left(\frac{z_{ref} + z_0}{z_0}\right)} \qquad k = 0.35$$

FØRTRAN:

```
ZREL = (ZREF + Z0)/Z0
USTAR = 0.35 * VWREF/ALØG(ZREL)
```

Boundary Layer Height:

$$z_{BL} = \frac{246\ \bar{u}_{ref}}{|\sin\phi| \log \frac{z_0 + z_{ref}}{z_0}}$$

FØRTRAN:

```
ZBL = 246. * VWREF/SIN(PHI)/ALØG 10(ZREL)
```

Geostrophic Wind:

$$V_G = \bar{u}_{ref}\left(\frac{z_{BL}}{z_{ref}}\right)^P$$

FØRTRAN:

```
VG = VWREF * (ZBL/ZREF)**P
```

Mean Wind (boundary layer):

$$\bar{u} = \bar{u}_{ref}\left(\frac{z}{z_{ref}}\right)$$

FØRTRAN:

```
VW = CVW*A**P
CVW = VWREF/ZREF**P
```

Mean Wind (free atmosphere):

$$\bar{u} = \bar{u}_{BL} + a(z - z_{BL})$$

FØRTRAN: VW = VGC + WS*A/FTS

VGC = VG-WS*ZBL/FTS

(FTS multiplication converts knots into ft/s.)

Wind Deviation from the Geostrophic Wind at the Top of the Surface Layer:

$$\alpha_{SL} = \text{Arcsin}\left[-10.7\,\frac{u_{*_0}}{V_G}\left(1 - \frac{z_{ref} - z_{SL}}{z_{BL}}\right)\right]$$

FØRTRAN: ALPSL = ASIN(10.7*WSTAR/VG*((ZREF-ZSL)/ZBL-1.))

Geostrophic Wind Heading:

$$\Psi_G = \Psi_{WO} - \alpha_{SL}$$

FØRTRAN: PSIWG = PSIWO-ALPSL

Wind Heading (boundary layer):

$$\alpha = \text{Arcsin}\left(\frac{z_{BL} - z}{z_{BL} - z_{SL}}\ \sin\alpha_{SL}\right)$$

FØRTRAN: PSIW = PSIWG + ASIN((ZBL-A)*CWBL)

CWBL = ALPSL/(ZBL-ZSL)

Wind Heading (free atmosphere):

$$\Psi_W = \Psi_G - b\left(\frac{|\ 180 - D_0|}{90} - 1\right)(z - z_{BL})$$

FØRTRAN:

```
PSIW = CPSIW*A+PSIW1

CPSIW = VRGFA*(1.-ABS(180-D0)/90.)/100./RAD

PSIW1 = -ZBL*CPSIW+PSIWG
```

(RAD multiplication converts radians into degrees.)

Program Description

1. Name: CONTROL

   Nature: MAIN PROGRAM

   Language: FORTRAN/ADEPT

   Call: —

   Inputs: BY COMMONS, SEE LISTING

   Outputs: —

   Externals: ABS, AMOD, ATAN, ITIME, SQRT

   Subroutines: BEACONS, DYNAMICS, INITRADAR, INITWIND, RTOF, SAMPLE $DIALS, $NHALT, $GRAFX

2. Name: INITRADAR

   Nature: SUBROUTINE

   Language: FORTRAN

   Call: CALL INITRADAR

   Inputs: XR, YR, SIGRGE, SIGBRG: PRINTED ON REQUEST

   Outputs: XR, YR, SIGRGE, SIGBRG by COMMON/PARAD/

   Externals: —

   Subroutines: —

3. Name: RADAR

   Nature: SUBROUTINE

   Language: FORTRAN

   Call: CALL RADAR

   Inputs: XR, YR, SIGRGE, SIGBRG by COMMON/PARAD/from INITRADAR

   Outputs: XMMES, YMES by COMMON/DISP/

4. Name: INITWIND

   Nature: SUBROUTINE

   Language: FORTRAN

   Call: CALL INITWIND

   Inputs: PHI, PSIMES, PSIWO, QFU10, VRGFA, VWMES, VWREF, WS, ZMES, ZTURB: printed on request

   Outputs: ZBL, ZSL, ZTURB, P, CVW, WS, VGC, USTAR, UT1, VT1, WT1, WTZ, PSIWO, PSIWG, PSIW1, CPSIW, CWBL: by COMMON/PARWD/

   Externals: ABS, ALOG, ASIN, SIN

   Subroutines: —

5. Name: WIND

   Nature: SUBROUTINE

   Language: FORTRAN

   Call: CALL WIND

   Inputs:
   - Parameters of COMMON/PARWD/ from INITWIND
   - XI, BETAG,A by COMMON/PRMTR/ from DYNAMICS
   - STTET, CTTET, SFIE, CFIE by COMMON/EXTRA/ from DYNAMICS
   - UVEL, VVEL, WVEL, VTOT by COMMON/WORK/ from DYNAMICS
   - T by COMMON/TIME/ from CONTROL

   Outputs: UWTOT, VWTOT, WWTOT by COMMON/WIND/

   Externals: ASIN, COS, EXP, SIN, SQRT

   Subroutines: GAUSS

6. Name: GAUSS

   Nature: SUBROUTINE

   Language: FORTRAN, ADEPT

6. Call: CALL GAUSS (XM, XSD, X)

   Inputs: XM (mean), XSD (standard deviation)

   Outputs: X : random variable of mean X and standard deviation XM

   Externals: –

   Subroutines: GAUSSIAN (ADEPT), included in GAUSS

7. DYNAMICS and other subroutines.
   The total wind components, UWTOT, VWTOT, WWTOT are sent to DYNAMICS from WIND by COMMON/WIND/.

   See FTL Memo M76-3 for a complete listing of ADAGE computer simulation of the nonlinear aerodynamics of the Boeing 707-320B used by the M.I.T. Flight Transportation Laboratory.

```
      SUBROUTINE INITRADAR
      COMMON/PARAD/XR,YR,SIGRGE,SIGBRG
      DATA RAD/57.296/
C     RADAR CHARACTERISTICS
      WRITE(10,100)
      READ(10,0)XR
      WRITE(10,200)
      READ(10,0)YR
C     STANDARD DEVIATIONS
      WRITE(10,400)
      READ(10,0)SIGRGE
      IF(SIGRGE.LT.1.)SIGRGE=185.
      WRITE(10,300)
      READ(10,0)SIGBRG
      IF(SIGBRG.LT..001)SIGBRG=.25
      SIGBRG=SIGBRG/RAD
100   FORMAT('  INPUT RADAR COORDINATES IN FEET'/
     1'  ORIGIN:RUNWAY THRESHOLD'/
     2'  X AXIS:RWY AXIS,DIRECTION OF LANDING'/'  X=?'/)
200   FORMAT('  Y=?'/)
300   FORMAT('  INPUT BEARING STANDARD DEVIATION IN DEGREES'/
     1'  IF UNKNOWN PRINT 0.(SELECTS 0.25 DEG)'/)
400   FORMAT('  INPUT RANGE STANDARD DEVIATION IN FEET'/
     1'  IF UNKNOWN,PRINT 0.(SELECTS 185 FT)'/)
      RETURN
      END
```

```
      SUBROUTINE RADAR
      COMMON/DISP/XMMES,YMES
      COMMON/PRMTR/V,XI,BETAG,DT
     COMMON/PRMTR/ALPHA,BETA,PHI,VX,VY,VZ,THETA,A,XM,Y,R,RIAS
      COMMON/PARAD/XR,YR,SIGRGE,SIGBRG
      DELTX=XM*6080.2-XR
      DELTY=Y-YR
      THETA=ATAN2(DELTY,DELTX)
      RHO=SQRT(DELTX**2+DELTY**2)
      CALL GAUSS(0,SIGRGE,ERR)
      RHO=RHO+ERR
      CALL GAUSS(0,SIGBRG,ERR)
      THETA=THETA+ERR
      XMMES=RHO*COS(THETA)/6080.2
      YMES=RHO*SIN(THETA)
      RETURN
      END
```

```
      PROGRAM INITWIND
      COMMON/PARWD/ZBL,ZSL,ZTURB,P,CVW,WS,VGC,USTAR,UT1,VT1
     1,WT1,WT2,PSIW0,PSIWG,PSIW1,CPSIW,CWBL
      DATA RAD/57.296/,FTS/1.71/
      DATA PI/3.141593/,S3/1.7320508/,T/1./
C     WIND CHARACTERISTICS
      Z0=0.15
C     REFERENCE WIND
      WRITE(10,400)
      READ(10,0)VWREF
      WRITE(10,401)
      READ(10,0)ZREF
      WRITE(10,402)
      READ(10,0)PSIW0
      PSIW0=PSIW0/RAD
C     AIRPORT DATA
      WRITE(10,500)
      READ(10,0)PHI
      WRITE(10,501)
      READ(10,0)QFU10
C     COMPUTATION OF LAYER CHARACTERISTICS
      PHI=PHI/RAD
      ZREL=(Z0+ZREF)/Z0
      USTAR=0.35*VWREF/ALOG(ZREL)
      ZBL=246.*VWREF/SIN(PHI)/ALOG(ZREL)*ALOG(10.)
      ZSL=300.
      WRITE(10,600)ZBL
C     TURBULENCE CHARACTERISTICS
      READ(10,0)ZTURB
      IF(ZTURB.LT.ZBL)ZTURB=ZBL
C     WIND MEAN PARAMETERS
      P=0.18
1001  VG=VWREF*(ZBL/ZREF)**P
      WRITE(10,700)VG
C     SUPPLEMENTARY DATA
      READ(10,0)ZMES,VWMES
      IF(ZMES.LE.ZREF)GO TO 1000
      VMSRF=VWMES/VWREF
      ZMSRF=ZMES/ZREF
      P=ALOG(VMSRF)/ALOG(ZMSRF)
      GO TO 1001
1000  CONTINUE
```

```
C       MEAN WIND FREE ATMOSPHERE
        WRITE(10,710)
        READ(10,0)WS
        IF(WS.LT.00001) WS=0.01
C       WIND VELOCITY PARAMETERS
        CVW=VWREF/ZREF**P
        VGC=VG-WS*ZBL/FTS
C       SHIFT ANGLE PARAMETERS
C       FREE ATMOSPHERE
        WRITE(10,720)
        READ(10,0)VRGFA
        IF(VRGFA.LT.0.0001)VRGFA=0.7
        D0=180+PSIW0*RAD
        IF(D0.GT.360.)D0=D0-360.
        ALPSL=ASIN(10.7*USTAR/VG*((ZREF-ZSL)/ZBL-1.)/RAD)
        PSIWG=PSIW0-ALPSL
        CPSIW=VRGFA*(1.-ABS(180.-D0)/90.)/100./RAD
        PSIW1=-ZBL*CPSIW+PSIWG
        CWBL=ALPSL/(ZBL-ZSL)
C       INITIALISATION
        UT1=0
        VT1=0
        WT1=0
        WT2=0
        RETURN
400     FORMAT('  INPUT SURFACE WIND CHARACTERISTICS'/
     1' VELOCITY IN KNOTS ?'/)
401    FORMAT('  HEIGHT OF MEASURE IN FEET ?'/)
402     FORMAT(' WIND HEADING(MAGNETIC) ?'/)
500     FORMAT('  AIRPORT LATITUDE IN DEGREES ? '/
     1'  IF UNKNOWN,WRITE 45.'/)
501    FORMAT('  MAGNETIC HEADING OF LANDING IN DEGREES ?'/)
600     FORMAT('  BOUNDARY LAYER HEIGHT : ',F10.0,'FT',/
     1'  IF TURBULENCE HIGHER WRITE HEIGHT,OTHERWISE WRITE 0.'/)
700     FORMAT('  GEOSTROPHIC WIND (TOP OF BOUNDARY LAYER): '/
     1/F10.0,' KTS,IF THIS VALUE SEEMS CORRECT AND/OR NO OTHER DATA'/
     2'  WRITE 0.,0. . OTHERWISE INPUT ANOTHER WIND MEASURE :'/
     3'  HEIGHT(FT),VELOCITY(KTS)'/
     4'  IN ALL CASES PRINT ONE DATA PER LINE'/)
710     FORMAT('  A VALUE OF 0.01S-1 IS TAKEN FOR WIND SHEAR IN FREE AT
     1PHERE'/' IF ANOTHER VALUE IS CHOSEN INPUT ITS VALUE IN S-1'
     2/'  OTHERWISE WRITE 0.'/)
720     FORMAT('  THE RATE OF VEERING IN FREE AMOSPHERE '/
     1'  IS CHOSEN EQUAL TO 0.7DEG/100FT'/
     2'  IF ANOTHER VALUE IS CHOSEN,INPUT ITS VALUE IN DEG/100FT'/
     3'  OTHERWISE PRINT 0.'/)
        END
```

```
      SUBROUTINE WIND
     COMMON/PARWD/ZBL,ZSL,ZTURB,P,CVW,WS,VGC,USTAR,UT1,VT1,WT1
    1,WT2,PSIWO,PSIWG,PSIW1,CPSIW,CWBL
     COMMON/TIME/T
      COMMON/PRMTR/VA,XI,BETAG,DT
      COMMON/PRMTR/ALPHA,BETA,PHI,UX,VY,VZ,THETA,A,XM,Y,R,RIAS
      COMMON/EXTRA/DDFIE,DDTET,DDSY,RFIE,RTET,RSY,STTET,CTTET
      COMMON/EXTRA/SFIE,CFIE
      COMMON/WORK/UVEL,VVEL,WVEL,VTOT,UDTT,VDTT,WDTT,VTOD
      COMMON/WIND/UWTOT,VWTOT,WWTOT
      DATA PI/3.14159/,S3/1.732/,FTS/1.71/,RAD/57.296/
C     MEAN WIND
      IF(A.LT.ZBL) GO TO 200
      VW=VGC+WS*A/FTS
      PSIW=CPSIWG*A+PSIW1
      GO TO 400
200   VW=CVW*A**P
      IF(A.LT.ZSL) GO TO 300
      PSIW=PSIWG+ASIN((ZBL-A)*CWBL)
      GO TO 400
300   PSIW=PSIWO
C     AXIS TRANSFORMATIONS(MEAN WIND:BODY AXES)
400   PSI=(XI-BETAG)/RAD
      CPSI=COS(PSI-PSIW)
      SPSI=SIN(PSI-PSIW)
      U=CPSI*CTTET*VW
      V=(CPSI*STTET*SFIE-SPSI*CFIE)*VW
      W=(CPSI*STTET*CFIE+SPSI*SFIE)*VW
      IF(A.LT.ZTURB) GO TO 500
C     TOTAL WIND IF NO TURBULENCE
      UWTOT=U
      VWTOT=V
      WWTOT=W
      RETURN
C     TURBULENCE
500   IF(A.GT.1750.) GO TO 600
      LV=A
      LH=145.*SQRT(A)
      GO TO 700
600   LH=1750.
      LV=1750.
```

```
700     SIGV=1.3*USTAR*(1.-A/ZTURB)
        SIGH=SIGV*(LH/LV)**.3333333*VTOT/SQRT(PI*LH)
        CUT1=EXP(-VTOT/LH*T)
        CALL GAUSS(0,SIGH,WN)
        UT=WN+UT1*CUT1
        UT1=UT
        CALL GAUSS(0,SIGH,WN)
        VT=WN+VT1*CUT1
        VT1=VT
        TINV=VTOT/LV
        SIGV=S3*VTOT/SQRT(2*PI*LV)*SIGV
        EXPN=EXP(-TINV*T)
        CWT1=2*EXPN
        CWT2=-EXPN**2
        CWN1=EXPN*TINV*(T*TINV*(1.-S3)-S3)*SIGV
        CALL GAUSS(0,SIGV,WN)
        WT=CWT1*WT1+CWT2*WT2+WN+CWN1*WN1
        WN1=WN
        WT2=WT1
        WT1=WT
C       AXIS TRANSFORMATIONS(TURBULENCE:BODY AXES)
        UTB=UT*CTTET-WT*STTET
        VTB=UT*STTET*SFIE+VT*CFIE+WT*CTTET*SFIE
        WTB=UT*STTET*CFIE-VT*SFIE+WT*CTTET*CFIE
C       TOTAL WIND
        UWTOT=U+UTB
        VWTOT=V+VTB
        WWTOT=W+WTB
        RETURN
        END
```

```
        SUBROUTINE GAUSS(X,V,Y)
        AR=X
        MD=V
A       ADEPT
JPSR GAUSSIAN
EXPUNGE
ENTRY:GAUSSIAN
GAUSSIAN: JUMP .
          ARXO'F
          ARMD U1
          NOOP
          MDAR NB
          MPYI 10065
          0
          MDAS'F 22063
          ARMD NC
          MDAR'A MSK
          ARAR'N'F
          MDAE NC
          ARMD NB
          ARAR'H'F
          ARRS 3
          MDAE U1
          ARMD U1
ENDR
          MDAR U1
          DIVI 26627
          0
          MDAR'A MSKU.
          ARMD U2
          MDIR GAUSSIAN
NB:       254366464
MSK:      77777!H
NC:       0
U1:       0
U2:       0
MSKU:     77777
TERMINATE
F       FORTRAN
        Y=GAUSSIAN
        RETURN
        END
```

References

Boussinesq, J. Theorie Analytique de la Chaleur, Vol. 2, Gauthiers-Villars, Paris, 1903.

Busch, N.E. "On the Mechanics of Atmospheric Turbulence," Workshop on Micrometeorology, American Meteorological Society, Boston, Mass., 1973.

Businger, J.A. "Turbulent Transfer in the Atmospheric Surface Layer," Workshop on Micrometeorology, American Meteorological Society, Boston, Mass., 1973.

Businger, J.A., Wingaard, J.C., Izumi, Y. and Bradley, E.F. "Flux-Profile Relationships in the Atmospheric Surface Layer," Journal of the Atmospheric Sciences, Vol. 28, 1971, pp. 181-189.

Calder, K.L. "In Classification of Shallow Layer Thermal Correction for a Compressible Fluid Based in the Boussinesq Approximation," Quarterly Journal of the Royal Meteorological Society, 94, 1968, pp. 89-92.

Chalk, K.L., Neal, T.P., Harris, F.E. and Pritchard, F.E. Background Information and User Guide for MIL-F-8785B (ASG), "Military Specification - Flying Qualities of Piloted Airplanes," Technical Report AFFDL-TR-69-72, 1969.

Clarke, R.H. and Hess, G.D. "Geostrophic Departure and the Functions A and B of Rossby-Humber Similarity Theory," Boundary Layer Meteorology, Vol. 7, 1974, pp. 267-287.

Corely, C.J. "A Simulation Study of Time Controlled Aircraft Navigation," S.M. Thesis, Dept. of Electrical Engineering, Massachusetts Institute of Technology, 1976.

de Moor, G. "La Turbulence dans la Couche Limite Atmospherique," La Meteorologie, June 1975, pp. 107-124; December 1975.

Dutton, J.A. and Fichtl, G.H. "Approximate Equations of Motion for Gases and Liquids," Journal of the Atmospheric Sciences, Vol 26, 1969, pp. 241-254.

Dyer, A.J. "A Review of Flux Profile Relationships," Boundary Layer Meteorology, Vol. 7, 1974, pp. 373-382.

Estogne, M.A. "Numerical Modeling of the Planetary Boundary Layer," Workshop Micrometeorology, American Meteorological Society, Boston, Mass., 1973.

Fiedler, F. and Panofsky, H.A. "Atmospheric Scales and Spectral Gaps," Bulletin of the American Meteorological Society, Vol. 51, No. 12, 1970, pp. 1114-1119.

Garrison, J.N. "An Assessment of Atmospheric Turbulence Data for Aeronautical Application," Royal Aeronautical Society, International Conference on Atmsopheric Turbulence Proceedings, 18-21 May, 1971.

Gifford, F.J. "The Interpretation of Meteorological Spectra and Correlations," Journal of Meteorology, 16, No. 3, 1959, pp. 344-346.

Haugen, D.A., Kaimal, J.C. and Bradley, E.F. "An Experimental Study of Reynolds Stress and Heat Flux in the Atmospheric Surface Layer," Quarterly Journal of the Royal Meteorological Society, Vol. 97, 1971, pp. 168-180.

Hemesath, N.B., Bruckner, J.M.H., Krippner, R.A., Meyer, D.H. and Murphy, J.W. "Three and Four Dimensional Area Navigation Study Simulation and System Development," Technical Report No. DOT-FA72WA-3123, 1974.

Kurkowski, R.L., Fichtl, G.H. and Gera, J. "Development of Turbulence and Wind Shear Models for Simulator Application," Vol. I, NASA, Aircraft Safety and Operating Problems Conference, NASA SP-270-1971.

Landau, L.D. and Lifshits, E.M. Fluid Mechanics, Pergamon Press, London, 1963.

Lax, F.M. "Design and Simulation of a Descent Controller for Strategic Four-Dimensional Aircraft Navigation," S.M. Thesis, Dept. of Electrical Engineering, Massachusetts Institute of Technology, 1975.

Lewellen, W.S. and Teske, M. "Prediction of the Monin-Obukhov Similarity Functions from an Invariant Model of Turbulence," Journal of the Atmospheric Sciences, Vol. 30, 1973, pp. 1340-1345.

Lumley, J.L. and Panofsky, H.A. "The Structure of Atmospheric Turbulence," Interscience Publications, New York-London-Sidney, 1964.

Matveev, L.T. Fundamentals of General Meteorology, Physics of the Atmosphere, Israel Program for Scientific Translations, NASA TT 67-5138, 1967.

MacCready, P.B. "Turbulence Measurements by Sailplane: The Inertial Subrange of Atmospheric Turbulence," Journal of Geophys. Research, 67, No. 3, pp. 1041-1059.

Melgarejo, J.W. and Deardorff, J.W. "Stability Functions for the Boundary Layer Resistance Laws Based Upon Observed Boundary Layer Heights," Journal of the Atmospheric Sciences, Vol. 31, No. 5, 1974, pp. 1324-1333.

Menga, G. and Sundarajan, N. "Stochastic Modeling of Mean Wind for In-Flight Wind Estimation," 1975.

Monin, A.S. and Yaglom, A.M. Statistical Fluid Mechanics, I, MIT Press, Cambridge, (Mass.) and London, (England), 1971.

Monin, A.S. and Yaglom, A.M. Statistical Fluid Mechanics, II, MIT Press, Cambridge, (Mass.) and London, (England), 1975.

Naylor, H.T., Balintfy, L.H., Burdick, S.D. and Chu, K. Computer Simulation Techniques, John Wiley and Sons, Inc., 1966.

Oberbeck, A. "Veber die Warmeleitung der Flussigkeiten bei Berucksichtigung der Stromungen infolge von Temperatur Differenzen," Ann. Physik, 7, 1879, pp. 271-292.

Panofsky, H.A. "Tower Micrometeorology," Workshop on Micrometeorology, American Meteorological Society, Boston, Mass., 1973.

Pitchard, F.E. "A Statistical Model of Atmospheric Turbulence and a Review of the Assumptions Necessary for its Use," AGARD Stability and Control, Part 2, September 1966, AD-665 320.

Priestley, C.H.B. "The Isotropic Limit and the Microscale of Turbulence," Adv. in Geophys., 6, (Atmospheric Diffusion and Air Pollution), 1959, pp. 97-100.

Rand Corporation. A Million Random Digits with 100,000 Normal Deviates, Free Press, New York, 1955.

Syono, S. and Gambo, K. "On Numerical Prediction, II," Journal of the Meteor Society of Japan, Ser. 2, 40, No. 3. 1952, pp. 127-135.

Tennekes, H. and Lumley, J.L. A First Course in Turbulence, MIT Press, Cambridge, (Mass.) and London, (England).

Tversoi, P.N. Physics of the Atmosphere, Technical Translation NASA TT 288, 1965.

Van der Hoven, J. "Power Specturm of Horizontal Wind Speed in the Frequency Range from 0.0007 to 900 Cycles per Hour," Journal of Meteorology, 14, No. 2, 1957, pp. 160-164.

Vinnichenko, N.K. "The Kinetic Energy Spectrum in the Free Atmosphere - 1 Second to 5 Years," Tellus XXII, No. 2, 1970, pp. 158-166.

Vinnichenko, N.K., Pinus, N.Z., Shmeter, S.M. and Shur, G.N. Turbulence in the Free Atmosphere, Consultants Bureau, New York, London, 1973.

Webb, E.K. "Profile Relationships: The Log-Linear Range, and Extension to Strong Stability," Royal Meteorological Society Quarterly Journal, Vol 96, 1970.

Wyngaard, J.C. "On Surface Layer Turbulence," Workshop on Micrometeorology, American Meteorological Society, Boston, Mass., 1973.

Zilitinkevich, S.S. "Shear Convection," Boundary Layer Meteorology, 3, 1973, pp. 416-423.